ESTABLISHMENT OF THE POTENTIAL OF FLAKE REINFORCED LAMINATES AS ENGINEERING STRUCTURAL MATERIALS

March 1962

Prepared under Navy, Bureau of Naval Weapons

Contract NOw 61-0305-c

Final Report

Covering period 1 January 1961 through 28 February 1962

NARMCO RESEARCH & DEVELOPMENT
A Division of Telecomputing Corporation
San Diego, California

ESTABLISHMENT OF THE POTENTIAL OF FLAKE REINFORCED LAMINATES AS ENGINEERING STRUCTURAL MATERIALS

March 1962

Prepared under Navy, Bureau of Naval Weapons

Contract NOw 61-0305-c

Final Report

Covering period 1 January 1961 through 28 February 1962

NARMCO RESEARCH & DEVELOPMENT
A Division of Telecomputing Corporation
San Diego, California

FOREWORD

This report was prepared by Narmco Research & Development, A Division of Telecomputing Corporation, under Navy Bureau of Weapons Contract NOw 61-0305-c. This study was initiated by the Materials Division of the Bureau to determine the suitability of flake reinforced composites as engineering structural materials. The investigation was administered by Mr. Paul Stone, Code RRMA-32, BuWeps, Washington 25, D.C.

This report covers work done between 1 January 1961 and 1 March 1962.

Included among those who cooperated in the research and the preparation of the report were: Leonard P. Suffredini, Manager, Product Engineering Department, Narmco Materials, A Division of Telecomputing Corporation; Bud L. Duft, Program Manager; Dr. S. Dharmarajan, Research Consultant; C. Y. Chia, Research Engineer; Norman Brink, Research Engineer; Jere Horsley, Research Technician; Dr. Steven Yurenka, Manager, Engineering Research; Dale Black, Manager, Application Engineering; and Curt Thompson, Research Engineer.

ABSTRACT

The fundamental structural properties investigated during the first year of the program were advanced in detail, and advantageous applications of flake composites were determined. Combinations of flake with glass fibers were tested and their structural potential is discussed.

The theoretical work conducted during the period covered by this report predicts inherent stress concentrations of up to eight times the nominal stress in circular flake composites.

The fabrication of cylinders and shapes other than flat plates using preformed, b-staged sheets of flake composite material and fluid molding pressure is reported to have advantages over other fabrication methods.

TABLE OF CONTENTS

Section		Page
	Introduction	1
I	Flake Fiber Combinations	3
	A. Fabrication of Test Specimens	3
	B. Test Procedures and Results	3
	C. Discussion of Test Results	14
	D. Potential of Flake Fiber Composites	15
II	Fabrication of Cylinders	17
	A. Inflatable Mandrel Method	17
	B. Filament Winding Under Tension	18
	C. Centrifugal Casting	19
	D. Hydroclave Method	21
III	Notch Sensitivity of Flake Reinforced Composites	23
	A. Notched Tensile Data	23
	B. Discussion of Notched Specimen Results	25
	C. Data on Specimens with a Hole	26
IV	Electrical Properties of Flake Composites	27
V	Cryogenic Tests	30
VI	Incorporation of Carbon Black Filler	31
VII	Thread Strength	32
VIII	Rocket Nozzle Erosion Rate	35

TABLE OF CONTENTS (Continued)

Section		Page
IX	Summary of Theoretical Investigations.	39
	A. The Determination of the Stresses in the Lap Joints of Circular Shaped Plates by the Method of Conformal Mapping.	39
	B. A Review of Theories of Solid and Composite Beams.	43
	C. A Comparitive Study of Ultimate Strength of a Given Composite Reinforced Either by Flakes or Fibers or by Flake-Fiber Combinations Under Bending and Compressive Loads.	44
X	Summary and Conclusions.	44
	Appendix - A Comparative Study of Ultimate Strength of a Given Composite Reinforced Either by Flakes or Fibers or by Fiber-Flake Combination Under Bending and Compressive Loads.	45

LIST OF FIGURES

Figure		Page
1	Key to Composite Descriptors	4
2	Layout of Test Specimens on 10" x 10" Laminates	5
3	Average Mechanical Properties of Glass Flake + 181 Glass Cloth	11
4	Average Mechanical Properties of Mica Flake + "Isotropic Scotchply"	12
5	Average Mechanical Properties of Glass Flake + "Unidirectional Scotchply"	13
6	Sketch of Flake-Fiber End Plate for a Battery Case	16
7	Filament Wound Battery Case	16
8	Cross Section of Assembly for Inflatable Mandrel Technique	17
9	Typical Glass Flake Cylinder	18
10	Filament Wound Flake Cylinder, 6" I.D.	19
11	Centrifugally Cast Test Specimen Failed in Edgewise Compression	20
12	One-Gallon Can Used for Centrifugal Casting of Flake Cylinders	20
13	A Centrifugally Cast Cylinder	21
14	Hydroclave Assembly	22
15	Notched Tensile Test Specimen	23
16	Maximum Stress at the Root of the Notch vs. Stress Concentration Factor K_t	25
17	Nominal or Average Stress at Failure vs. Stress Concentration Factor K_t	25

LIST OF FIGURES (Continued)

Figure		Page
18	Test Specimen for Stress Concentration Studies, $K_t \triangleq 2.0$	26
19	Variation in Nominal Stress at Failure of a Specimen With a Stress Concentrator vs. the Radius of the Concentrator for $K_t = 2.00$	28
20	Thread Shear Test Specimen	32
21	View of Threads in a Glass Flake Composite	33
22	Load/Thread vs. Bolt Diameter	36
23	H_2 - O_2 Rocket Nozzle Tests, Throat Diameter Erosion	37
24	H_2 - O_2 Rocket Nozzle Tests, Throat Erosion Rate	38
25	Stress Distribution Along the Circular Arc NMLKI	40
26	Radial Forces Applied to Lap Joints of a Unit Circular Plate and the Plate With Transition Curve as a Part of its Edges	41
27	Stress Concentration in Small Overlap Angle	42
28	Failure Pattern of Small Overlap Angle	42
29	Stress Concentration in Large Overlap Angle	43
30	Three Types of Composites	47

LIST OF TABLES

Table		Page
I	Tension Data On Glass Flake + 181 Cloth	6
II	Flexure Data On Glass Flake + 181 Cloth	6
III	Compression Data On Glass Flake + 181 Cloth	7
IV	Tension Data On Mica Flake + "Isotropic Scotchply"	7
V	Flexure Data On Mica Flake + "Isotropic Scotchply"	8
VI	Compression Data On Mica Flake + "Isotropic Scotchply"	8
VII	Tension Data On Glass Flake + "Unidirectional Scotchply"	9
VIII	Flexure Data On Glass Flake + "Unidirectional Scotchply"	9
IX	Compression Data On Glass Flake + "Unidirectional Scotchply"	10
X	Compression Data On Centrifugally Cast Flake Plugs	19
XI	Stress Concentration Factor Data	24
XII	Notched Tensile Specimen Results	24
XIII	Dielectric Strength of Large Area of Mica Flake Composite	27
XIV	Dielectric Strength of Selected Areas of Mica Flake Composite	29
XV	Arc Resistance Time	29
XVI	Arc Resistance Voltage Breakdown Ratio	30
XVII	Comparison of Mica Flake with Glass Flake	30
XVIII	Flexural Strength of Four Flake Specimens at -320°F	31

LIST OF TABLES (Continued)

Table		Page
XIX	A Comparison of the Properties of Flake Laminates With and Without Carbon Black	32
XX	Thread Strength in Glass Flake Laminate 70-30 Flake Laminate - .36" Thick	34
XXI	Thread Strength in Glass Flake Laminate Laminate Thickness = 0.68".	34
XXII	Thread Strength in Aluminum Plate	35
XXIII	Comparison of Maximum Compressive Loads in Different Composite.	49
XXIV	Comparison of Maximum Bending Moments in Different Composites	52

INTRODUCTION

During the first year of this 26 month program the efforts were slanted toward determining the fundamental Engineering properties of flake reinforced plastics. Certain serious criticisms of flake composites as a structural material arose during this period. Among these are their inherently low tensile strength and poor moldability of anything but thin flat plates. These properties having been well established and adequantely explained, the last portion of the program which is described in this report was devoted to the development of the established assets and a search for new assets or promising structural applications of flake composites.

As a result of these investigations, it appears as if flake composites have their place as an engineering structural material. Although this material is not a good molding compound, it can be treated as a laminating material in the form of thin preformed sheets. Whereas the tensile strength is low, the compressive strength is fair. Perhaps the most notable observation, however, was the compressive and flexural strengths and moduli of combinations of glass flake and glass fiber composites.

These properties were somewhat anomalous, since they were higher in some cases than for either the flake or fiber composites alone. Fabrication variables were held to a minimum in these tests in order to obtain valid comparisons.

The significance of flake fiber composites is that the attractive features of each material can be combined. These features (see Section I) make flake fiber combinations particularly suitable to underwater structures. Much of the traditional criticism of the use of glass reinforced plastics as a structural hull for underwater vehicles (e.g., water permeability, machinability) can be resolved by this material; however, further tests and refinements of fabrication procedures are necessary before its acceptance as an engineering design material.

Because flake has potential as a compressive material, it was decided to evaluate the material for use as a submersible structure. To do this, methods for molding flake into cylinders were developed. The techniques considered and described in Section III fall into the following categories:

1. Centrifugal casting
2. Filament winding under tension
3. Inflatable mandrel
4. Hydroclaving

The concept behind Item 1. is self explanatory. Category 2. consists of winding pre-tensioned glass roving over a heated, cylindrical flake preform. The tension in the roving provides the pressure required to remove the air from the composite and to completely wet the flakes with resin. Technique 3 consists of laying-up a flake preform against a cylindrical mandrel made of high

temperature elastomer. The outer surface of the cylindrical preform is covered with a steel shim and clamped with a large hose clamp. Then the assembly is placed in an oven and the mandrel is hydraulically pressurized to provide molding pressure. In Technique 4, a flake preform is formed on a cylindrical mandrel. A thin polyvinyl (PVA) cylinder is placed against the inside surface of the mandrel and another against the outside surface of the flake preform. The two PVA cylinders are sealed together at the top and bottom to form a cylindrical bag. The assembly is placed into a hydraulic pressure chamber. The bag is evacuated and then hydraulic pressure is applied. Then the bag is vented to the atmosphere and the entire chamber is heated to cure temperature.

The most promising technique is that of hydroclaving; however, capabilities for this procedure were not in existance until the closing phases of this program, and the one attempt at hydroclaving a flake cylinder was unsuccessful due to leak in the PVA bag.

After having established that a given material is strong and stiff and can be fabricated into various shapes, one may well ask whether it can be machined. Is it affected structurally by holes, notches or other discontinuities? To some extent these questions have been answered for flake composites, but not for flake fiber combinations. Flake composites have exhibited relatively low sensitivity to holes and notches in the material (Section II). It has been hypothesized that this property is due to the presence of inherent stress concentrators. In an analysis of load transfer from flake to flake, it has been shown that stress concentrations of up to eight times the average stress may occur in flake overlap areas (see Section IX). Thus, stress concentrations of two to three times the average stress due to holes or notches may be insignificant in comparison to the inherent concentrators. Thus it is believed that flake reinforced composites will offer excellent secondary structures such as appurtenance and opening load transfer mechanisms in structures of composite materials. Areas such as access holes, ports, etc. in rocket motor cases, torpedos and other structural shells require such load transfer systems.

In addition to the above, flake composites offer excellent electrical properties. The dielectric strengths of glass and mica flake composites are compared in Section V.

Other areas of investigation include: flexural strength at cryogenic temperatures; the effect of carbon black filler included in the resin matrix; thread strength; and rocket nozzle erosion rate.

Areas of theoretical investigation include: an analysis of the stresses in circular lap joints using conformal mapping; a review of theories of solid and composite beams; and flake and fiber theory.

I. FLAKE FIBER COMBINATIONS

Theoretical and experimental analyses were conducted to determine the advantages of combining glass and mica flake with glass fiber composites for the purpose of improving the composite properties in general. Considerable advantage appeared to be gained by the proper utilization of flake and fiber, e.g., the insensitivity to notches, holes or other machining and the water impermeability of flake, and the strength of fiber composites.

A. Fabrication of Test Specimens

The glass flake used in these tests and all other tests involving glass flakes was 10-35 mesh, two micron Owens-Corning Filmglas, and was laminated with 30% by weight of epoxy resin X-270. The mica flake was 10-35 mesh low grade muscovite.

The fiber portion of the composites were of three varieties - 181 glass cloth with an X-270 epoxy binder; Minnesota Mining & Manufacturing Type 1002 "Isotropic Scotchply" and "Unidirectional Scotchply". The Scotchply is fiber sheet impregnated with a b-staged epoxy. The Isotropic material is a three layer material. Each layer consists of continuous, non-woven, parallel glass fibers and the fibers of each layer are oriented at 60° to the fibers of each of the other layers. The unidirectional material consists of one layer of continuous, non-woven, parallel glass fibers.

The flake fiber composites were fabricated by laminating the desired number of flake preforms or b-staged sheets with sheets of the glass fiber material, and then compression molding the lamination into a flat 10" x 10" plate at 800 psi molding pressure and at 350°F cure temperature for two hours. After cure, each layer of flake composite and each layer of fiber composite were between 0.02" and 0.03" thick in all laminates.

The combinations of flake and fiber investigated are sketched and alphabetical descriptors of each configuration are given for the purpose of identification in Figure 1. Test specimens were cut from the 10" x 10" laminates as shown in Figure 2.

B. Test Procedures and Results

Tensile, flexure and compression tests were run on the flake fiber combinations. These tests were run in compliance with Mil. Spec. LP-406. The results of the tests are given in Tables I through IX. These results are presented in graphical form in Figures 3, 4, and 5. Since the standard deviation of test values of up to six specimens is not very meaningful, only the range of these test values is presented. The extremes of the ranges are shown in Figures 3, 4, and 5 as short horizontal lines. The flexure specimens of configuration B were loaded so that the flake side was in compression and the fiber side in tension.

A - Flake alone

5 layers of flake

B - Flake & Fiber on bottom

4 layers of flake
1 layer of fiber

C - Flake & Fiber in middle

4 layers of flake
1 layer of fiber

D - Flake & Fiber at 1/3 points

3 layers of flake
2 layers of fiber

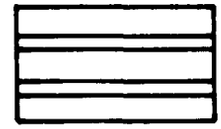

E - Flake & Fiber on top & bottom

3 layers of flake
2 layers of fiber

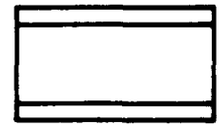

F - Flake & Fiber on top, middle & bottom

2 layers of flake
3 layers of fiber

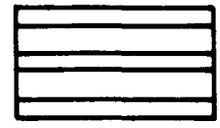

G - Flake & five layers of fiber distributed uniformly

4 layers of flake

H - Fiber alone

5 layers of fiber

Figure 1. Key to Composite Descriptors

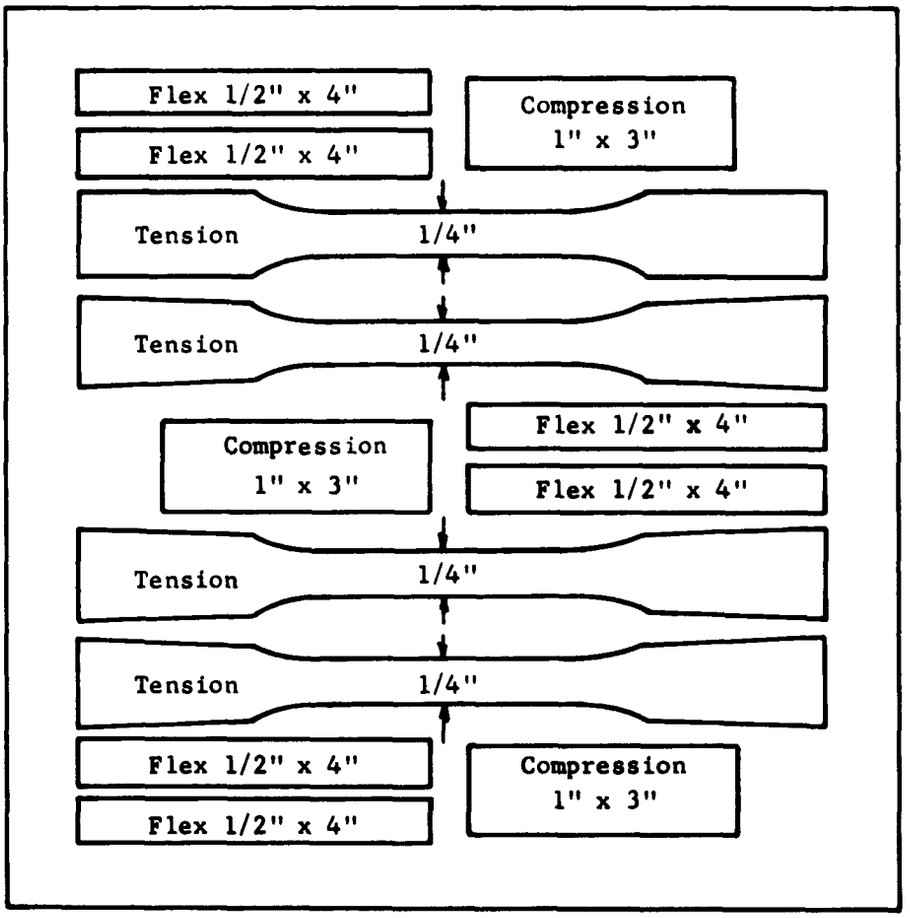

Figure 2. Layout of Test Specimens on 10" x 10" Laminates

TABLE I

TENSION DATA ON GLASS FLAKE + 181 CLOTH

Specimen Descriptors	No. of Specimens Tested	Maximum Strength (PSI)	Average Strength (PSI)	Maximum Modulus (PSI x 10^{-6})	Average Modulus (PSI x 10^{-6})
A	4	25,600	20,100	6.39	5.44
B	4	17,700	16,300	6.48	4.85
C	5	25,400	22,500	5.62	4.81
D	5	21,800	19,600	4.57	4.22
E	4	20,500	19,600	5.03	4.11
F	4	22,700	22,500	4.75	4.52
G	4	40,800	36,500	5.34	4.86
H	4	73,500	72,500	4.85	4.26

TABLE II

FLEXURE DATA ON GLASS FLAKE + 181 CLOTH

Specimen Descriptors	No. of Specimens Tested	Maximum Strength (PSI)	Average Strength (PSI)	Maximum Modulus (PSI x 10^{-6})	Average Modulus (PSI x 10^{-6})
A	6	38,000	32,900	6.22	5.87
B	5	70,700	67,200	4.84	4.61
C	6	44,700	39,400	5.82	5.68
D	6	49,500	41,300	5.41	5.02
E	6	77,200	71,300	3.41	3.39
F	3	87,400	77,500	4.46	4.23
G	6	47,800	45,100	4.23	3.98
H	6	71,500	65,700	4.25	4.06

TABLE III

COMPRESSION DATA ON GLASS FLAKE + 181 CLOTH

Specimen Descriptors	No. of Specimens Tested	Maximum Strength (PSI)	Average Strength (PSI)	Maximum Modulus (PSI x 10^{-6})	Average Modulus (PSI x 10^{-6})
A	3	53,700	52,700	6.07	5.92
B	3	43,400	38,500	5.29	5.17
C	3	68,500	61,500	5.44	5.28
D	3	59,200	49,900	5.05	4.90
E	3	53,500	49,900	4.63	4.56
F	3	61,800	57,800	4.91	4.56
G	3	79,700	78,500	4.62	4.37
H	3	63,700	59,200	4.06	3.87

TABLE IV

TENSION DATA ON MICA FLAKE + "ISOTROPIC SCOTCHPLY"

Specimen Descriptors	No. of Specimens Tested	Maximum Strength (PSI)	Average Strength (PSI)	Maximum Modulus (PSI x 10^{-6})	Average Modulus (PSI x 10^{-6})
A	4	11,900	8,900	13.46	12.06
B	4	11,600	10,600	9.20	8.78
C	4	10,600	9,100	8.96	8.30
D	4	20,700	18,600	8.33	7.32
E	4	20,900	18,100	9.21	8.70
F	4	30,500	27,200	7.23	6.69
G	4	29,200	24,800	8.56	7.27
H	6	81,000	70,100	6.77	5.22

TABLE V

FLEXURE DATA ON MICA FLAKE + "ISOTROPIC SCOTCHPLY"

Specimen Descriptors	No. of Specimens Tested	Maximum Strength (PSI)	Average Strength (PSI)	Maximum Modulus ($PSI \times 10^{-6}$)	Average Modulus ($PSI \times 10^{-6}$)
A	6	26,700	21,800	10.87	10.59
B	3	25,700	24,900	6.52	5.86
C	3	22,600	22,000	9.44	8.87
D	6	24,300	22,000	7.45	7.06
E	6	30,800	26,000	5.58	5.24
F	3	44,600	42,900	5.74	5.04
G	6	36,200	34,400	5.33	5.07
H	6	95,700	84,000	3.46	3.24

TABLE VI

COMPRESSION DATA ON MICA FLAKE + "ISOTROPIC SCOTCHPLY"

Specimen Descriptors	No. of Specimens Tested	Maximum Strength (PSI)	Average Strength (PSI)	Maximum Modulus ($PSI \times 10^{-6}$)	Average Modulus ($PSI \times 10^{-6}$)
A	3	25,400	20,900	10.42	10.33
B	3	19,000	18,300	8.24	8.12
C	3	22,100	20,800	8.00	7.83
D	3	21,900	21,600	7.54	6.70
E	3	22,300	21,300	7.17	6.82
F	3	22,700	22,000	5.79	5.66
G	3	23,600	22,700	6.39	5.90
H	6	51,500	45,200	2.83	2.75

TABLE VII

TENSION DATA ON GLASS FLAKE + "UNIDIRECTIONAL SCOTCHPLY"

Specimen Descriptors	No. of Specimens Tested	Maximum Strength (PSI)	Average Strength (PSI)	Maximum Modulus ($PSI \times 10^{-6}$)	Average Modulus ($PSI \times 10^{-6}$)
A	4	20,800	19,800	5.14	5.04
B	4	25,500	23,900	5.26	5.00
C	4	26,900	24,800	5.46	5.34
D	4	52,300	43,300	5.81	5.47
E	4	52,000	45,100	5.37	5.08
F	4	91,850	86,100	6.28	6.07
G	4	90,400	87,500	5.41	5.29
H	4	97,420	91,400	5.55	5.21

TABLE VIII

FLEXURE DATA ON GLASS FLAKE + "UNIDIRECTIONAL SCOTCHPLY"

Specimen Descriptors	No. of Specimens Tested	Maximum Strength (PSI)	Average Strength (PSI)	Maximum Modulus ($PSI \times 10^{-6}$)	Average Modulus ($PSI \times 10^{-6}$)
A	6	40,800	38,000	5.57	5.40
B	6	103,200	94,800	5.69	5.61
C	6	41,300	38,900	5.63	5.45
D	6	104,300	76,500	5.65	5.60
E	6	137,700	125,700	6.10	5.78
F	6	168,800	141,300	6.05	5.99
G	6	134,800	127,100	5.67	5.49
H	6	158,300	152,600	5.46	5.37

TABLE IX

COMPRESSION DATA ON GLASS FLAKE + "UNIDIRECTIONAL SCOTCHPLY"

Specimen Descriptors	No. of Specimens Tested	Maximum Strength (PSI)	Average Strength (PSI)	Maximum Modulus (PSI x 10^{-6})	Average Modulus (PSI x 10^{-6})
A	3	67,400	63,100	6.25	5.86
B	3	69,000	61,900	6.10	5.82
C	3	62,200	60,600	6.22	6.02
D	3	62,800	61,600	6.30	6.15
E	3	71,300	70,000	5.88	5.72
F	3	83,200	73,900	6.49	6.38
G	3	103,800	89,900	6.20	6.02
H	3	88,000	80,100	5.85	5.73

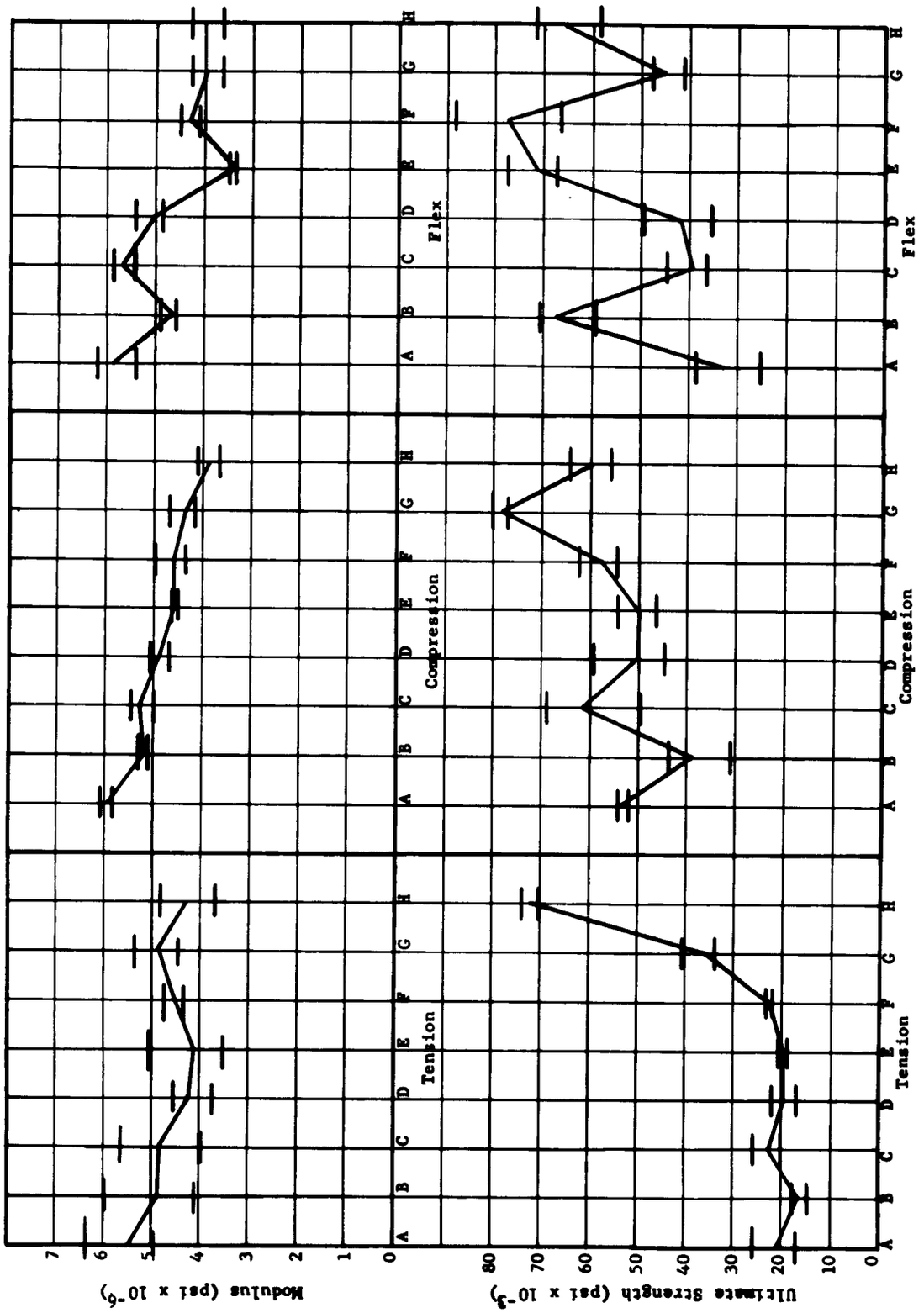

Figure 3. Average Mechanical Properties of Glass Flake + 181 Glass Cloth (With Indicated Range)

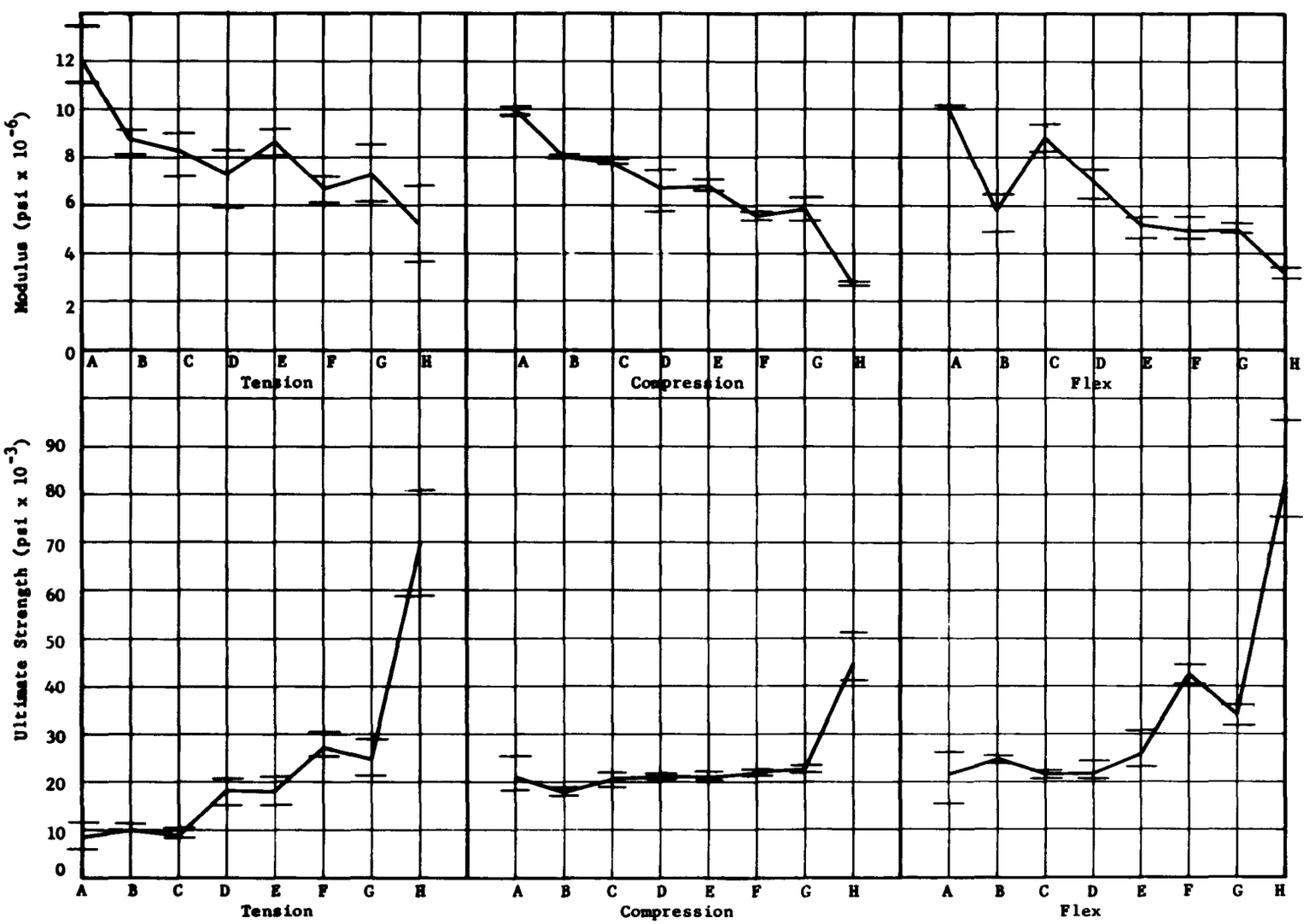

Figure 4. Average Mechanical Properties of Mica Flake + "Isotropic Scotchply"

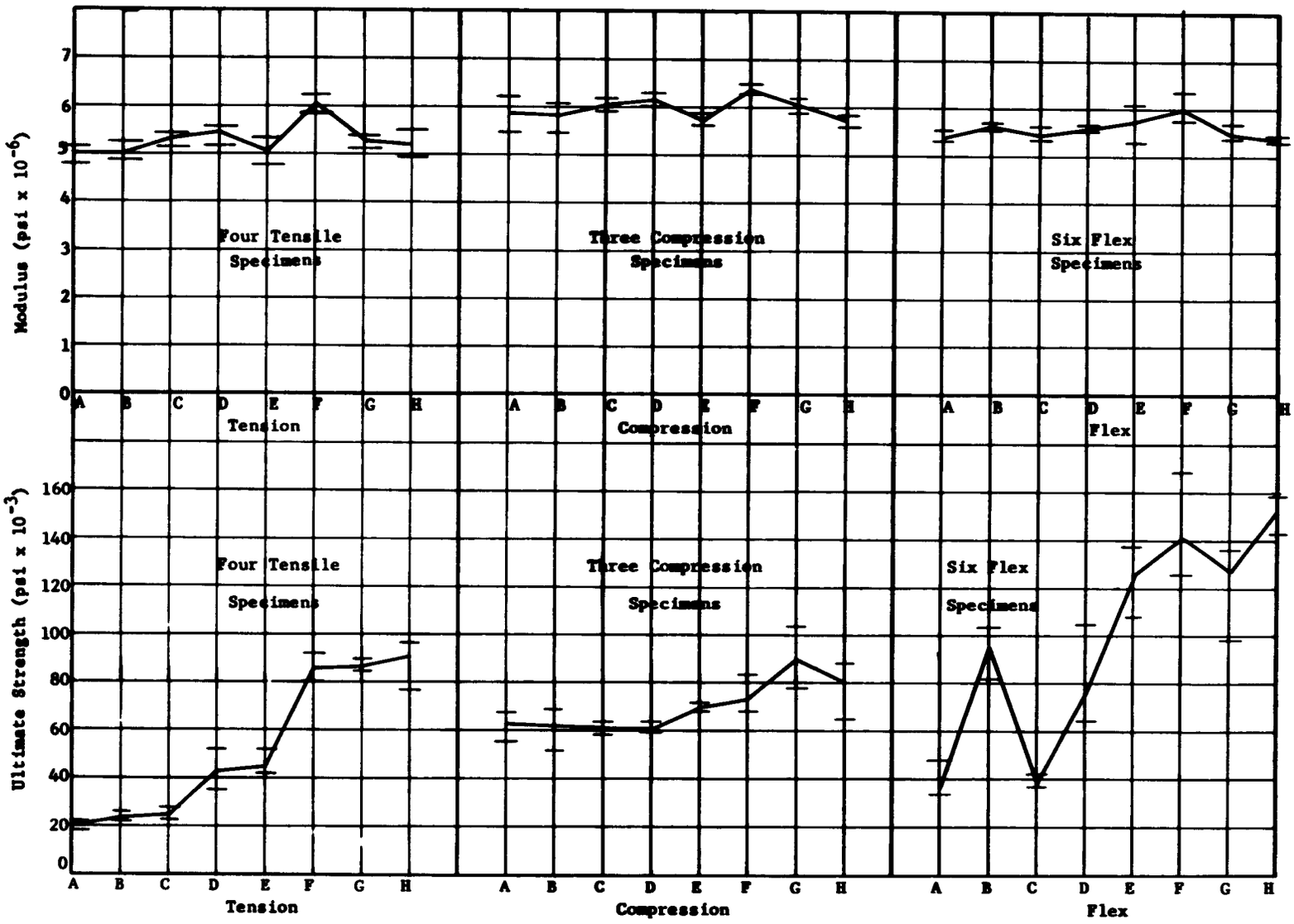

Figure 5. Average Mechanical Properties of Glass Flake + "Unidirectional Scotchply" (With Indicated Range)

C. Discussion of Test Results

1. Glass Flake + 181 Glass Cloth

The results of these tests are listed in Tables I, II, and III. A comparison of the data is shown in Figure 3.

It can be seen from the data that the flexural strength of either the glass cloth or the flake alone can be increased by combining the two into a composite laminate. The highest increase was obtained with configuration F. These specimens yielded an average strength increase of 135% over the glass flake control, and 17.9% over the glass cloth control.

The compressive strengths of the composite laminates also showed higher values than either of the controls in certain configurations. The highest laminate yielded 48.9% and 32.7% increases over flake and cloth, respectively. Specimens C yielded a 16.8% increase over flake and a 3.9% increase over cloth.

The tensile strength tests showed that an increase of 8.2% over the flake control specimens is attainable using the 9-layer sandwich laminate, G. All laminates containing flake had a lower tensile strength than did the cloth laminate; however, these flake cloth combinations have at least bidirectional strength properties. It is possible that the strength properties are nearly omnidirectional in the plane of the laminations due to the omnidirectionality of flake reinforced plastics in the plane of the flakes.

The moduli of the flake cloth laminates in almost all cases were greater than that of the cloth control laminate.

2. Mica Flake + "Isotropic Scotchply"

The results of these tests are listed in Tables IV, V, and VI. A comparison of the data is shown in Figure 4.

These materials were laminated in an effort to combine the high rigidity of mica flake and the high strength of glass fiber. The large strength increases for glass flake + glass fiber combinations were not observed in mica flake + glass fiber combinations. This was probably due to the poor quality of the mica flake. The mica used was a low quality muscovite. It is felt that further work in this field is justifiable, since high quality mica is now available with sufficient slenderness ratio (i.e., diameter to thickness ratio) to provide effective reinforcement. The modulus of mica is in the neighborhood of 25 million psi as compared to 10.5 million for E-glass.

3. Glass Flake + "Unidirectional Scotchply"

The results of these tests are listed in Tables VII, VIII, and IX. A comparison of the data is shown in Figure 5.

The highest average flexural strength and modulus for a combination was for configuration F - 141,300 psi strength and 5.99 x 10^6 psi modulus. One flex specimen of this group yielded an ultimate flexural stress of 168,800 psi. The average flexural strength for all combinations was lower than that of the fiber composite; however, the moduli for all combinations were higher than the moduli of both the flake and the fiber controls.

The compressive strength of specimens G was about 12% higher than that for the fiber control and 43% higher than for the flake control. The modulus was higher than the control moduli for most flake fiber combinations.

The tensile strengths for this series of flake fiber combinations were encouraging. Configuration G yielded 87,500 psi as compared to 91,400 psi for the fiber control. Again, the moduli of the combination specimens were consistently higher than for either material.

Configuration F seemed to have the best overall properties, consistently yielding the highest modulus and good strength properties.

D. Potential of Flake Fiber Composites

It is apparent from this data, that flake fiber composites have suitable engineering properties for applications which require low density, impermeability, and a respectable modulus as well as high strength. The highest strengths for flake fiber combinations are in compression and flexure, which suggests their application as an external pressure vessel.

The modulus property is an important parameter for these applications, in that instability and buckling is frequently the criterion for failure of an external pressure vessel. Fiberglass composites containing hollow fibers have a high specific strength (strength-to-density ratio); however, the modulus of such a material is inferior to composites of solid fibers and flake fiber combinations. In addition, both solid and hollow fiber composites are permeable to water. Pressure, osmotic, and dialytic forces cause "weeping" and water transferral from the outside to the inside along a relatively short resin path. The resin path is much longer and torturous for the same thickness of flake composite.

A flake fiber combination has already found application in another government program at Narmco (Contract No. A7289(NAS 5-1431)). The requirement was for end plates for a filament wound battery case. The plates had to be highly impermeable to the electrolytic solution and also have high biaxial flexural strength due to internal pressurization. A flake laminate disc with an outside layer of glass cloth was used (see Figures

6 and 7). This configuration withstood an internal pressure of 500 psi, at which point failure occured in another portion of the case. The maximum tensile stress as a result of biaxial flexure at 500 psi internal pressure was calculated to be 67,000 psi. Without the fiber layer, a flake end plate of the same thickness failed at 130 psi. (18,000 psi maximum stress.)

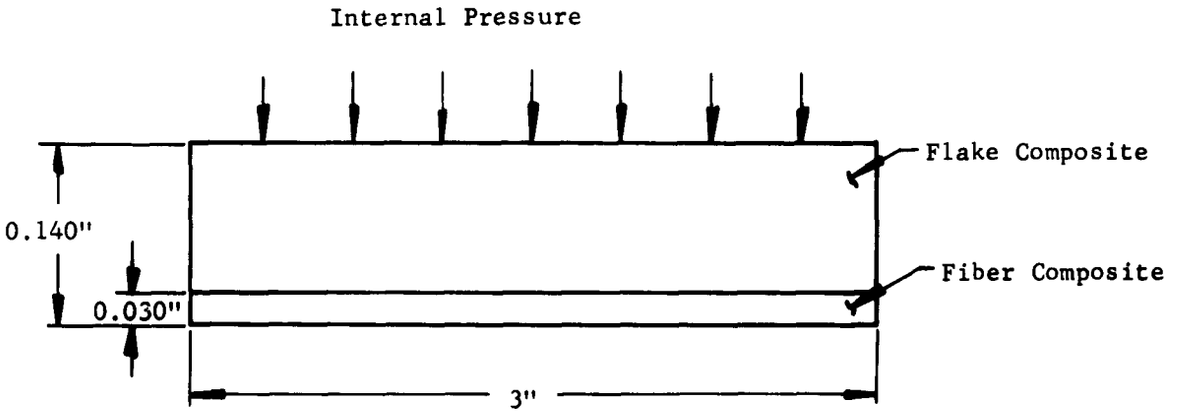

Figure 6. Sketch of Flake-Fiber End Plate for a Battery Case

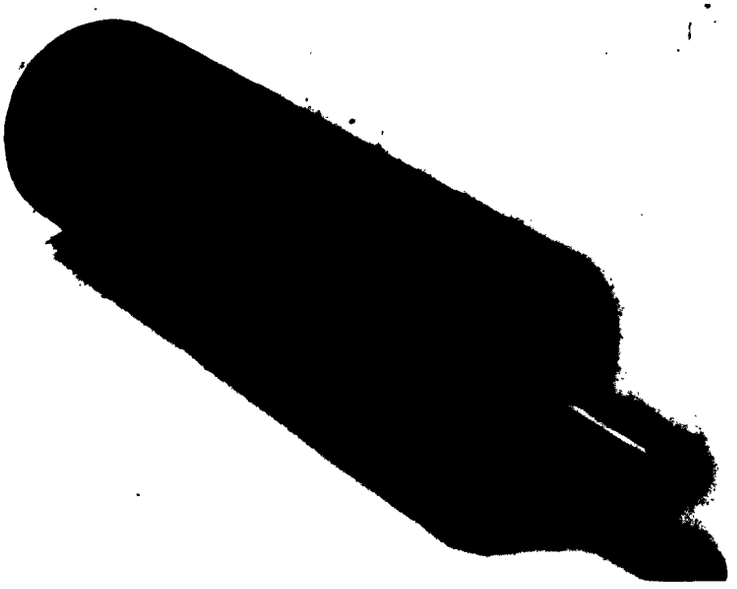

Figure 7. Filament Wound Battery Case

Even if flake fiber combinations are only as strong and as stiff as fiber composites, the properties of flake warrant its consideration for certain applications. Specifically, the combination of flake with filament winding requires investigation. The following section describes the problems and possibilities of combining flake with filament winding in a cylinder.

II. FABRICATION OF CYLINDERS

In an effort to determine whether flake or flake fiber composites can be formed into anything but flat plates, techniques for the fabrication of cylinders were investigated. In addition, the potential of flake for use in a submersible structure required the establishment of techniques for molding flake into cylinders. The four techniques considered are summarized below.

A. Inflatable Mandrel Method

The tool used in this method consists of a high temperature silicone cylinder (4.25" O.D.) with metal end plates (see Figure 8). One endplate is equipped with a hydraulic pressure fitting which will accept the pressure hose from a hand operated hydraulic pump. A flake preform was heated and bent around the mandrel. The preform was of sufficient length to afford a 1" overlap. A 0.010" stainless steel shim was wrapped over the part and clamped against the endplates with a large hose clamp. Then the mandrel was pressurized and heated to cure temperature.

The main difficulty encountered was that the elastomeric mandrel, being very soft, extruded between the shim and the endplate, precluding the application of sufficient molding pressure to the flake part.

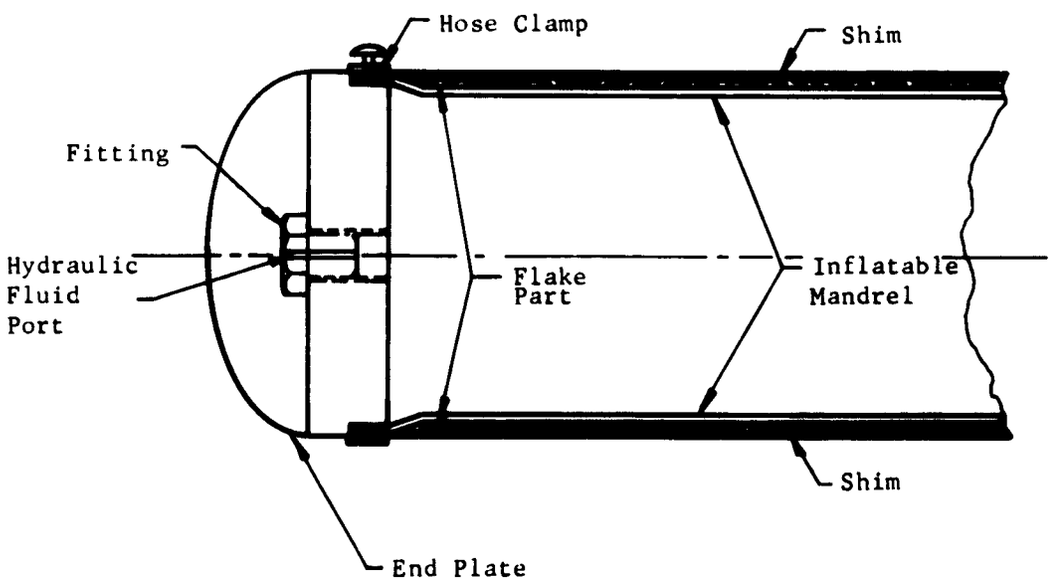

Figure 8. Cross Section of Assembly for Inflatable Mandrel Technique

However, the pressure did reach 150 psi for one cylinder, resulting in a partially translucent cylinder. None of the cylinders fabricated by this method were tested since they appeared dry, at least in spots, (see Figure 9) and there was insufficient flow to level the preform overlap.

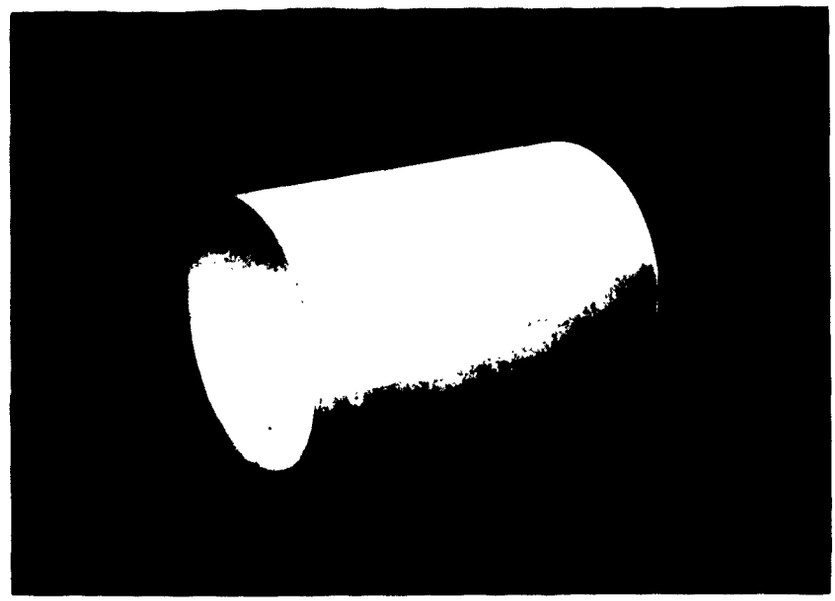

Figure 9. Typical Glass Flake Cylinder

B. Filament Winding Under Tension

In this method, a flake preform is heated and bent around a 6" O.D. spl mandrel. Thirty-end glass roving was then impregnated with a liquid epoxy resin and wound over the preform, warmed by a heated air gun. Th heat gun produced a temperature of about 300°F at the surface of the cy inder. The roving was wound under 10 pounds of tension. After two lay ers of roving were wound, the cylinder was post-cured and removed from the mandrel.

The physical appearance of the flake portion of the cylinder was poor (see Figure 10) in that the flakes did not appear to have been wetted the resin; however, flake alignment was good.

The preform overlap areas can be seen in Figure 9 as variations of the thickness of the cylinder. If the filaments had been wound under suff cient tension, flow would occur at these joints and they would disappe Accordingly, another cylinder was fabricated with filament tension in- creased to 15 pounds. This cylinder was broken in removing it from th mandrel; however, flow at the joints did not improve.

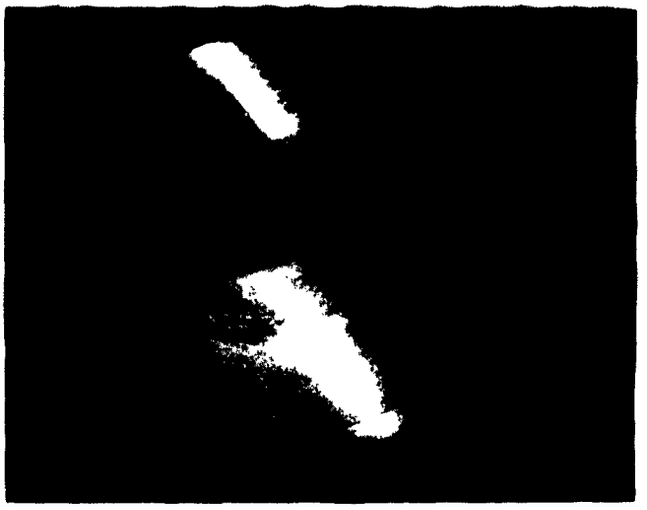

Figure 10. Filament Wound Flake Cylinder, 6" I.D.

C. Centrifugal Casting

One method of fabricating flake cylinders with no joints is centrifugal casting. The feasibility of this method was tested in a test tube centrifuge, 12" in diameter. Each of two 1" diameter polyethylene test tubes were filled about halfway with Shell's Epon 815 epoxy resin catalyzed with 14 parts per hundred diethylenetriamine (DTA). This resin has a low viscosity.

The tubes containing the resin mixtures were spun in the centrifuge at full speed (approx. 3000 rpm) to remove any suspended air bubbles. Dry glass flake was added and the tubes spun again at full speed until the flake fell to the bottom of the liquid resin (about 1/2 min). More flake was added and sedimented until sufficient flake had entered the resin. The centrifuge was then heated with a heated air gun until the resin cured. The resulting composite plug was machined into a cube (approximately 0.7" on each side). The cubes were tested flatwise (perpendicular to flakes) and edgewise (parallel to flakes) in compression. The data are summarized in Table X.

TABLE X

COMPRESSION DATA ON CENTRIFUGALLY CAST FLAKE PLUGS

	Flatwise		Edgewise	
	Average Strength	Average Modulus	Average Strength	Average Modulus
Glass Flake	39,000 psi	1.69×10^6 psi	25,900 psi	5.53×10^6 psi
Mica Flake	--	--	17,200 psi	4.03×10^6 psi

The flake content of the test specimens ranged from 56% to 70% by weight. The poor edgewise strength was due to poor flake alignment, as shown in Figure 11. This is a photograph of a test specimen after failure in edgewise compression. Flake alignment near the edges of the plugs was almost parallel to the walls of the test tubes.

Figure 11. Centrifugally Cast Test Specimen Failed in Edgewise Compression

The centrifugal casting of complete flake reinforced tubes was then attempted. The composite material was poured into a 1-gallon tin can with a cast polyester liner, to provide a smooth cylindrical surface. The bottom of the can was bolted to a milling machine along with an inside and outside aluminum back-up plate to strengthen the can (see Figure 12).

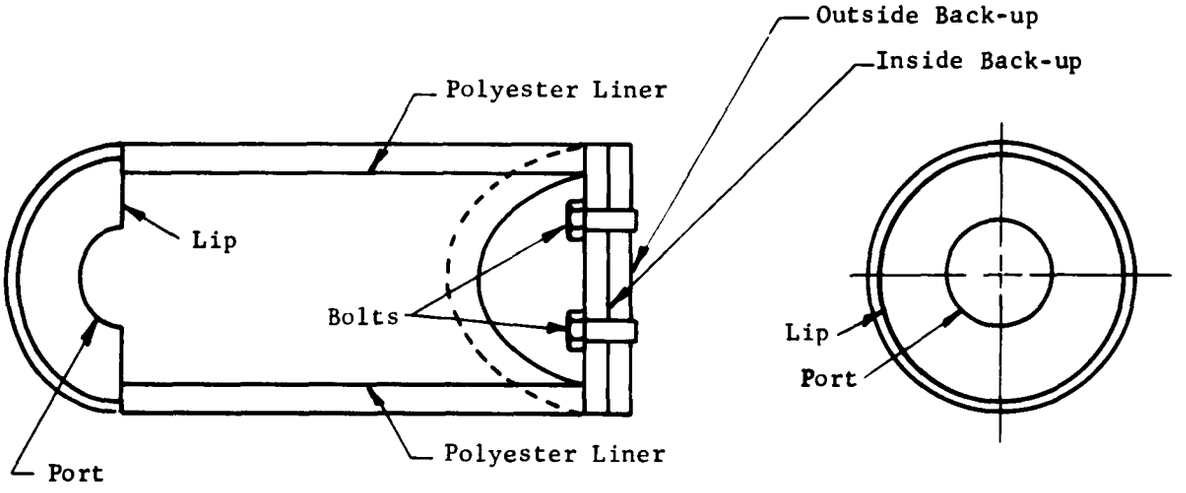

Figure 12. One-Gallon Can Used for Centrifugal Casting of Flake Cylinders

The spinning speed was 2450 rpm. The resin used was initially the 815-DTA system, used for plugs; however, this system polymerized too rapidly to get enough flake in the resin. The catalyst benzyldimethylamine (BDMA) was used with Epon-815, since this system requires much longer to cure (six parts BDMA per 100 parts 815). The catalyzed resin was entered into the spinning can through the port. The glass flake was sprinkled slowly onto the resin and, when no more flake would enter into the resin, a heated air gun was held in the port until the resin gelled (approximately 30 min). The part and container were removed from the milling machine and heated to 350°F for 2 hours. One cylinder is pictured in Figure 13. Flake orientation is, at best, fair, and attainable flake content at this spinning speed is only 55% by weight. This is attributable to the low angular velocity and radius (about 5.5") compared to those of the centrifuge. In fact, the acceleration in the centrifuge is about 1600 g's and in the spinning can it is about 600 g's. About 4300 rpm would be necessary to attain 1600 g's in the can.

Figure 13. A Centrifugally Cast Cylinder

One centrifugally cast cylinder was tested under compression in Narmco's hydraulic pressure chamber. Hoop stress at failure was only 9,580 psi.

Nevertheless, this is a promising technique for the fabrication of flake cylinders and it is felt that further work should be conducted at the required g-levels.

D. Hydroclave Method

In this method, once again the technique of wrapping a heated flake preform over a cylindrical mandrel is utilized. Then a PVA cylinder is placed against the inside surface of the mandrel and another PVA cylinder is placed on the outside surface of the flake part. The two PVA cylinders are heat sealed, or sealed with zinc chromate putty, at the top and

bottom to form a cylindrical bag around the part and mandrel (see Figure 14). The bag is evacuated and subjected to 800 psi hydraulic molding pressure. Then the bag is vented to the atmosphere and the entire assembly is heated to 350°F for two hours.

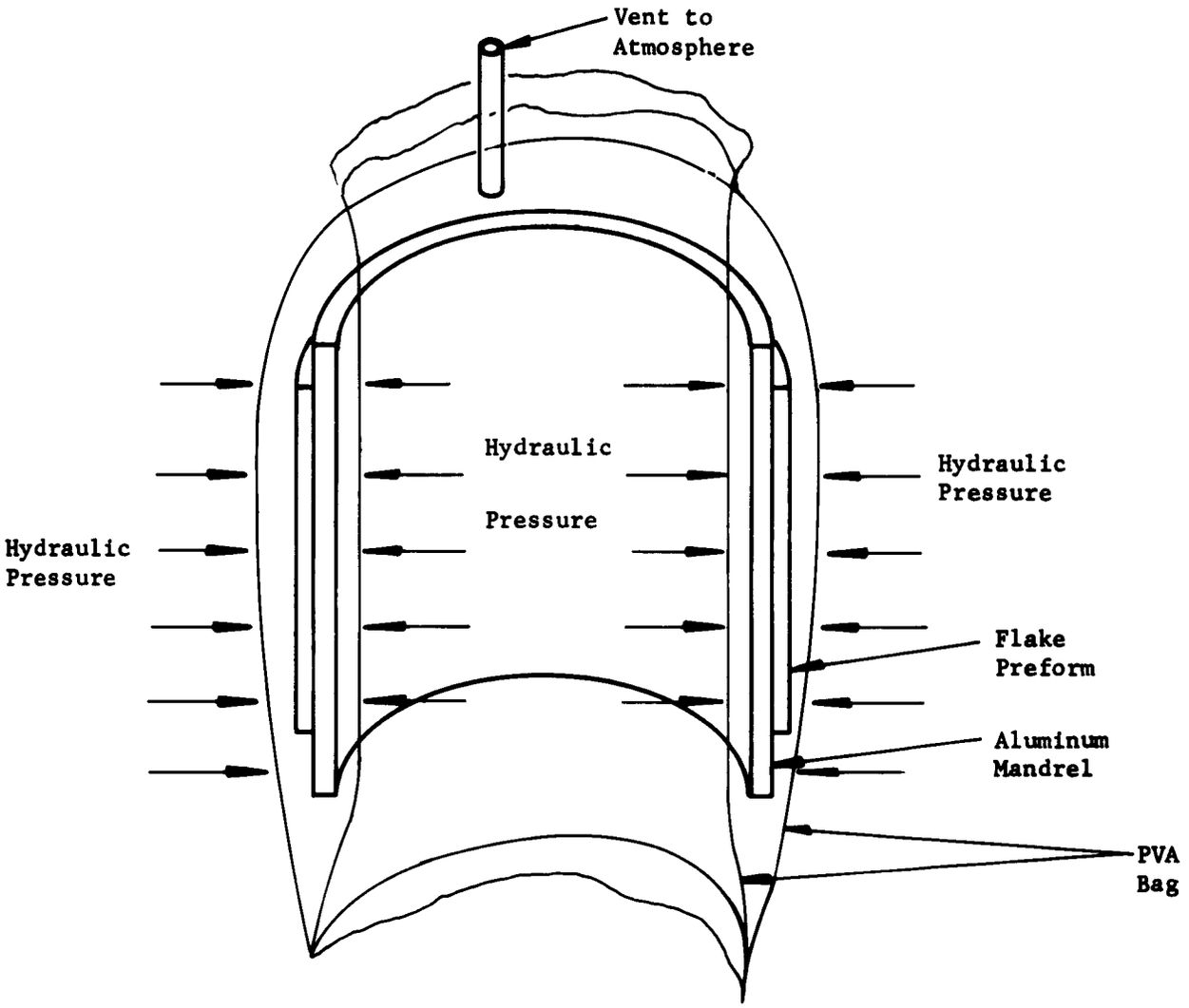

Figure 14. Hydroclave Assembly

The one attempt to fabricate a cylinder using this method was unsuccessful, due to a leak in the PVA bag. No further attempt was made since laboratory activity on this program ended shortly after the first effort. However, it is felt that this method offers the most promise of the four considered, since sufficient molding pressure is assured and it is adaptable to the combination of flake with filament winding.

III. NOTCH SENSITIVITY OF FLAKE REINFORCED COMPOSITES

Brittle materials are often characterized by their notch sensitivity. It is often a sufficient criteria for brittleness to simply view the stress-strain curve of a material and note the absence of any ductile or plastic behavior, in which case notch sensitivity can be expected. In the case of glass flake reinforced plastics the stress-strain curves show no evidence of inelastic strain up to a failing stress, and brittle behavior may be expected. Detailed examination, however, reveals that the composite is composed of two phases - a discontinuous glass phase surrounded by a continuous plastic matrix. Moreover, the reason for the apparent linearity of the stress-strain curve to failure lies in the fact that the glass flakes have large slenderness ratios. The bonded area is so large that the average shear stress and consequent shear strain in the resin gluelines are small.

In practical laminates the strain contribution attributable to the resin is less than 0.1% of the total strain. This argument breaks down at very low glass content, but is supported by the fact that the modulus of a practical flake laminate is simply the volume fraction of glass multiplied by the modulus of the glass. Thus, although the gross stress-strain behavior of the flake composite can be determined by integrating the average contribution of the simple flake to flake bonds, little can be said about the detailed stress-strain distribution in and around the individual randomly dispersed flake. It is, therefore, not a matter of a prior prediction to decide the manner in which a crack, starting at the root of a notch, will propagate a failure path through a flake composite. Indeed we may anticipate built-in stress raisers due to local inhomogeneities in glass and resin composition which will initiate failure independent of some arbitrarily induced notch.

The following investigation has been conducted for the purpose of examining the effect of the random distribution of flake, as found in practical flake laminates, on the ultimate strength of the composite.

A. Notched Tensile Data

One dozen 10" x 10" x 0.125" flake laminates were prepared using 70% by weight 2 micron Filmglas and an experimental proprietory resin, X-207. The glass flakes were screened, and the glass between 10 and 35 mesh used. One hundred dog-bone tensile specimens were cut from these laminates and pooled for test. Twelve specimens were selected at random and provided the value for the average ultimate tensile strength. Groups of eight specimens were then selected at random and notched as shown in Figure 15.

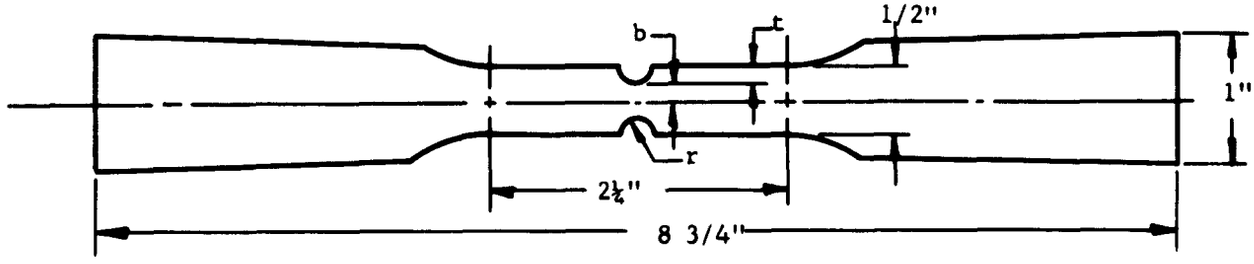

Figure 15. Notched Tensile Test Specimen

The following data was taken from the nomographs of Seeley & Smith (1) and used to calculate the value of b, t, and r required for a given stress concentration factor K_t. These data are shown in Table XI.

TABLE XI

STRESS CONCENTRATION FACTOR DATA

K_t	$\sqrt{\frac{t}{r}}$	$\sqrt{\frac{b}{r}}$	b inches	t inches	r inches
1.5	1.5	0.92	0.068	0.182	0.081
2.0	1.5	1.55	0.129	0.121	0.053
3.0	1.5	2.80	0.194	0.056	0.025
3.7	1.5	4.25	0.223	0.027	0.012

The data in the first three columns are taken from the nomographs. The last three columns are calculated values using the additional constraint

$$2\,b + 2\,t = 1/2$$

K_t is defined as the ratio of the stress at the root of the notch to the nominal stress in the adjacent cross section.

Eight specimens were tested under each of the notched conditions shown in Table VI. The average results along with the standard deviation of these tests are shown in Table XII.

TABLE XII

NOTCHED TENSILE SPECIMEN RESULTS

Stress Concentration Factor K_t	Nominal Cross Sectional Area sq. in.	Nominal Stress $\pm\sigma$ psi x 10^3	K_t x Nominal Stress $\pm\sigma$ psi x 10^3
1.0 (no notch)	0.063	22.0 ± 2.1	22 ± 2.1
1.5	0.018	21.3 ± 1.0	32.0 ± 1.5
2.0	0.033	19.5 ± 0.7	39.0 ± 1.4
3.0	0.050	16.0 ± 1.0	48.0 ± 3.0
3.7	0.056	15.7 ± 0.8	58.0 ± 3.0

(1) Seeley & Smith, Advanced Mechanics of Material. Page 391, Wiley & Sons.

B. Discussion of Notched Specimen Results

The data in Table XII, has been plotted in Figures 16 and 17, which show the manner in which the calculated maximum stress and the nominal stress change with the stress concentration factor introduced by the notch.

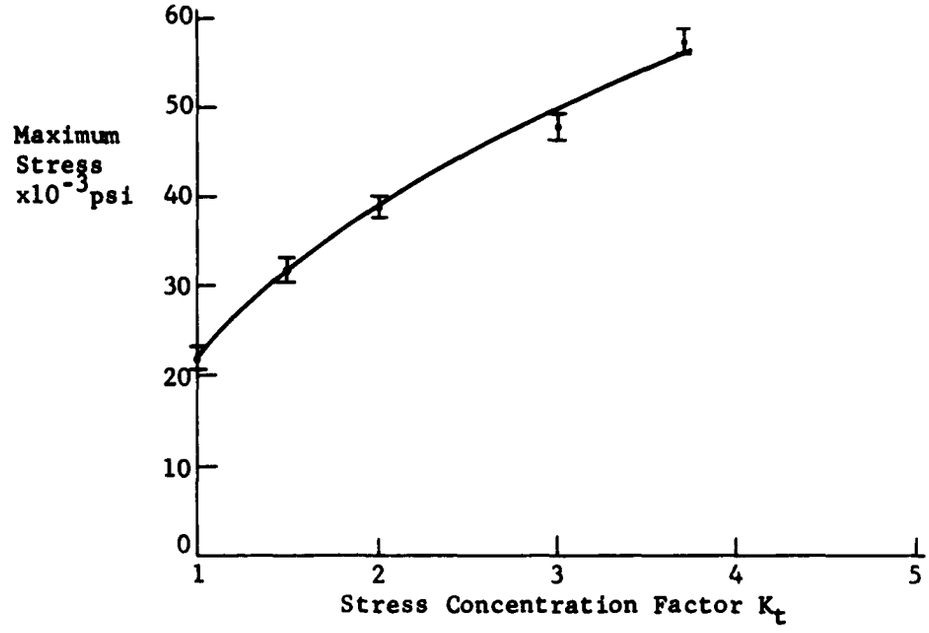

Figure 16. Maximum Stress at the Root of the Notch vs. Stress Concentration Factor K_t

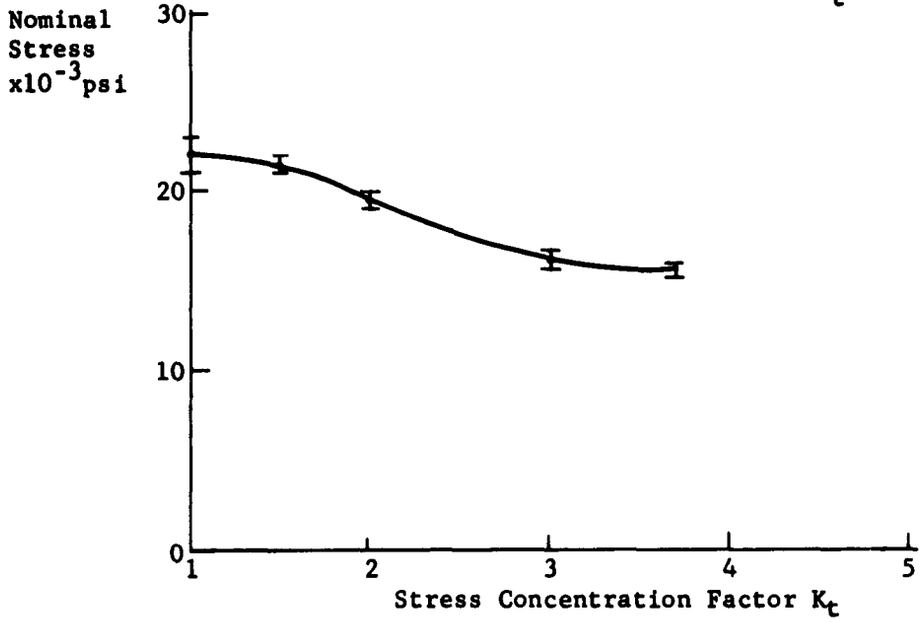

Figure 17. Nominal or Average Stress at Failure vs. Stress Concentration Factor K_t

Figure 16 shows that the calculated stress at the root of the notch continually increases as the notch becomes more severe. One will observe that the higher stress levels correspond to smaller sections of the flake laminate. Although in principle the maximum stress is concentrated at a line for any radius, still the notch with the larger radius allows a somewhat freer choice of positions of almost equal stress along which a crack may propagate. The analogy drawn is that materials when tested in small volume produce higher ultimate strength values than when tested in bulk.

The ultimate tensile strengths of flake laminates as calculated from uniaxial tension, pure bending and flexure are 22,000 psi, 31,000 psi and 40,000 psi, respectively. The area under maximum stress decreases in the same order as shown. Whether or not this analogy is valid for the notched specimen was investigated by testing a group of specimens bearing large holes with varying diameter at a constant stress concentration factor.

An interesting result is observed in Figure 17, where the nominal stress is plotted versus K_t. It is apparent that the nominal stress reaches the unnotched ultimate strength until a stress concentration having a factor of 1.5 to 2 is introduced. The specimen fails at the notched section because it is the minimum cross section. However, the fact that the nominal stress equals the ultimate strength would indicate that within a flake laminate there exists inherent stress raisers having associated with them a stress concentration factor of at least 1.5.

C. Data on Specimens with a Hole

The initial tests were run on specimens with notches with radii of 0.05" or less. This work was extended to specimens with central holes of diameters up to 1.25" (see Figure 18). The reason for this further work was to broaden the region of stress concentration to encompass many flakes.

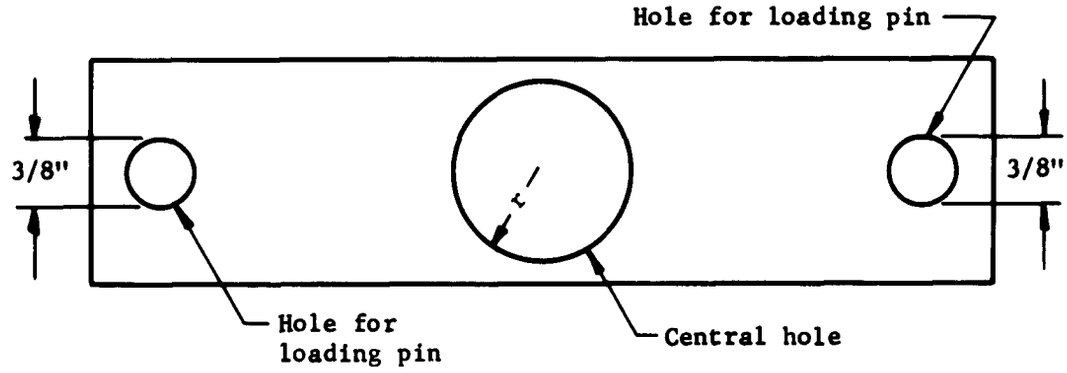

Figure 18. Test Specimen for Stress Concentration Studies, $K_t \cong 2.0$

The diameter of the central hole was always at least 88% of the total width of the specimen, resulting in a K_t very near 2.0 (between 2.00 and 2.03). The nominal stress in the narrow area of the specimens at failure is given in Figure 19, plotted versus the radius of the hole. The data from the notched dog-bone tests are also included, in which case the abscissa represents the notch radius.

While some decrease in the nominal stress at failure is noted, it is not as great as predicted since these concentrators should result in a nominal stress at failure of about 10,000 psi, according to the theory.

We are now left with only two alternatives. Either the concentrated stresses produced by the holes and notches considered are still within the region of one flake and do not undergo the costly process of transferral from flake to flake, or some other mechanism, as yet untheorized, distributes these concentrated loads.

IV. ELECTRICAL PROPERTIES OF FLAKE COMPOSITES

The electrical properties of commercial grade mica flake composites were evaluated for the purpose of comparison with those of glass flake reinforced composites. Test methods used were similar in important details to the Federal Specification L-P-406b and comparable ASTM methods as listed below:

Measurement	Fed. Spec. No.	ASTM Spec.
Dielectric constant and loss tagent at one megacycle, using the resonant rise-susceptivity variation method	4021	D150-42t
Dielectric stiength at power line frequencies (60 cycles)	4031	D149-40t
Arc Resistance	4011.2	D495-48t

The dielectric strength of the mica flake laminate was measured as described above. The result is presented in Table XIII. The results of the routine tests are greatly influenced by the distribution of flaws and foreign material in the commercial grade of mica.

TABLE XIII

DIELECTRIC STRENGTH OF LARGE AREA OF MICA FLAKE COMPOSITE

Sample Condition	Dielectric Strength volts/mil	Avg Dielectric Strength volts/mil
Untreated	494, 355, 404, 385, 327, 473	407
After 2 hours in boiling water	115, 103, 202, 314, 218, 280 156, 770*, 700*	198

* Excluded from the average

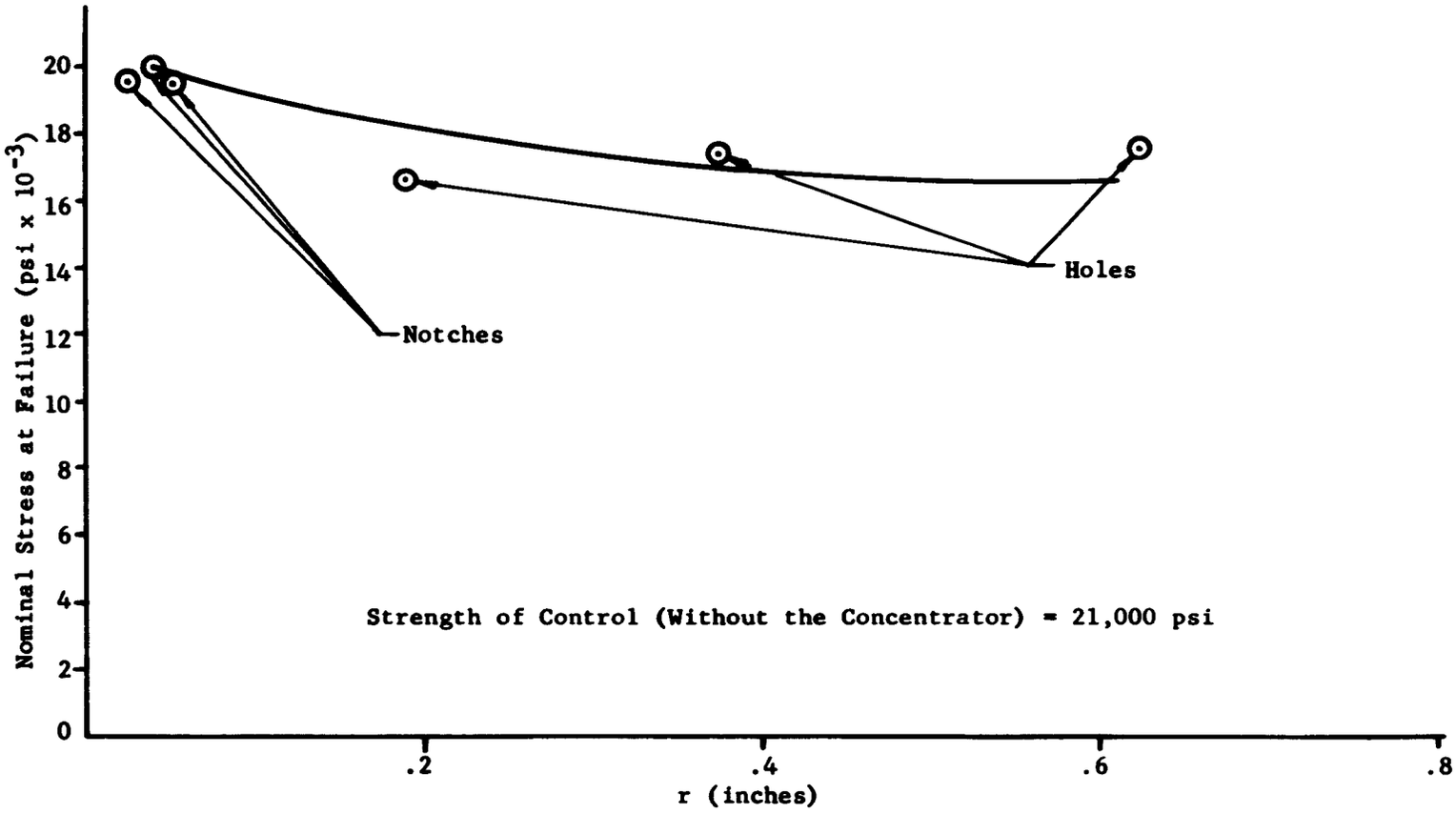

Figure 19. Variation in Nominal Stress at Failure of a Specimen With a Stress Concentrator vs. the Radius of the Concentrator for K_t = 2.00

Because of the great effect of these flaws, additional special measurements were performed, using Mylar film masks over the material, and testing a small area to voltage breakdown. The purpose of these tests was to determine the true dielectric strength of the mica flake reinforced composite, without including the effects of flaws and foreign materials. Each test was repeated until the arc occurred within the 1/2"-square area selected. A complicated pattern of electrical breakdowns occurred before the area in question was ruptured. The voltage gradient at each of the breakdowns, through the composite material outside the selected area, is listed in Table XIV.

TABLE XIV

DIELECTRIC STRENGTH OF SELECTED AREAS OF MICA FLAKE COMPOSITE

Test Area	Dielectric Strength Volts/Mil
#1	1090, 1001, 1080, 1150, 1080, 1200, 1080*
#2	746*
#3	965, 1290, 1320, 1270, 1260*
#4	280*

** Electrical rupture occurred through the sample area chosen

The results of these selected tests indicate that the dielectric strength is very dependent on uniformity of material structure and that selection of uniform regions in the sample materials was not better than 50% successful, on the basis of optical inspection. Dielectric strength as high as 1200 volts per mil was observed in selected regions of testing.

Arc resistance time and voltage breakdown ratios were evaluated. The results are presented in Tables XV and XVI.

TABLE XV

ARC RESISTANCE TIME

Sample Condition	Arc Resistance Time - Seconds	Average
Untreated	245, 243, 301, 254	261
After 2 hours in boiling water	242, 299, 242, 192	244

TABLE XVI

ARC RESISTANCE VOLTAGE BREAKDOWN RATIO

Sample Condition	V_1	V_2	V_2/V_1	Remarks
Untreated	5554	215	.039	
	5575	15	.0028	Average = .0137
	5575	15	.0029	
	5575	57	.0102	
After 2 hours in boiling water	5575	15	.0028	
	5700	15	.0026	
	5575	15	.0028	Average = .00279
	5575	300	.054*	

* Excluded from the average

The above evaluations indicate that mica flake is, in most cases, an excellent material for use in electrical applications. Pure forms of mica, eliminating the foreign matter, should indicate good consistent electrical properties. Table XVII presents a comparison of glass flake with mica flake.

TABLE XVII

COMPARISON OF MICA FLAKE WITH GLASS FLAKE

Property	Mica Flake	Glass Flake
Dielectric Strength V/mil		
a. Untreated	407, 1128*	1100
b. After 2 hours in boiling water	198,	816
Arc Resistance Time, secs.		
a. Untreated	261	199
b. After 2 hours in boiling water	244	202

* Selected test areas eliminating flaws and impurities

The above data indicate that pure mica composites will be as good as glass flake composites electrically.

V. CRYOGENIC TESTS

Limited data were obtained on the strength and modulus of glass flake composites in flexure at -320°F. The data are summarized in Table XVIII.

A slight increase over room temperature properties is evident, but they are not significant increases.

TABLE XVIII

FLEXURAL STRENGTH OF FOUR FLAKE SPECIMENS AT -320°F

Identification	Ultimate Strength (PSI)	Modulus ($PSI \times 10^{-6}$)
1	36,200	6.10
2	41,000	6.51
3	38,700	--
4	44,100	--
Average Values	40,100	6.31

VI. INCORPORATION OF CARBON BLACK FILLER

It was discovered that the inclusion of equal parts of carbon black by weight in epoxy resins increased the compressive strength of the resin by about 60% and the compressive modulus by about 40%. The density of the carbon black is between 1.8 and 2.0 gm/cm^3. Subsequently, a method was devised by which carbon black could be included in the dry powdered resin used in the fabrication of flake composites.

A batch of solid epoxy resin was melted and catalyzed. Then an equal weight of carbon black was stirred in the resin until the mixture was uniform. The filled resin was solidified and pulverized. Only that pulverized resin which passed through a 100-mesh screen was used to fabricate flake laminates.

Control laminates were made with no carbon black. The data are summarized in Table XIX. Tensile strength was not determined, due to the small size of the laminates.

The high modulus of carbon black-filled composites is probably due to the substitution of low modulus resin with high modulus carbon black.

The significant point in the data, however, is that the significant increases in modulus are not bought at the price of a reduction in strength. In point of fact, the average flexural strength increased with the inclusion of carbon black.

TABLE XIX

A COMPARISON OF THE PROPERTIES OF FLAKE LAMINATES
WITH AND WITHOUT CARBON BLACK

	Flake No Carbon Black	Flake With Carbon Black
Maximum Flexural Strength	35,700 psi	36,900 psi
Average Flexural Strength	33,400 psi	35,600 psi
Maximum Flexural Modulus	5.73×10^6 psi	6.88×10^6 psi
Average Flexural Modulus	5.60×10^6 psi	6.62×10^6 psi
Maximum Compressive Strength	49,100 psi	48,500 psi
Average Compressive Strength	45,200 psi	43,700 psi
Maximum Compressive Modulus	6.31×10^6 psi	6.96×10^6 psi
Average Compressive Modulus	5.96×10^6 psi	6.82×10^6 psi

VII. THREAD STRENGTH

An evaluation was made to determine the load-carrying capabilities of a threaded glass flake laminate. A laminate with a 70-30 glass flake - epoxy resin ratio was fabricated and several holes of different sizes were drilled and tapped with standard coarse bolt thread (see Figure 20). The thread sizes tested included

1/2 - 13
3/8 - 16
1/4 - 20
10 - 24 (3/16")

Figure 20. Thread Shear Test Specimen

For comparison, the same sized holes were drilled and tapped in a 2024-T4 aluminum alloy plate. The threads were tested by the "push through" method, that is, a standard bolt was threaded into the hole and loaded on the bolt head by a test machine. The threads in the glass flake laminate were of the same or better quality than that shown in Figure 21.

Figure 21. View of Threads in a Glass Flake Composite

The results of the tests are given in Tables XX, XXI, and XXII and shown in Figure 22. The calculated curve was based on the ultimate tensile strength of the material. The calculated load per thread was found by

$$\text{Load/thread} = \sigma_u \pi D_p d$$

where: σ_u = Ultimate tensile strength

D_p = Pitch diameter of bolt

d = Depth of thread

The test points were found by dividing the total thread load by the number of threads in the laminate. The limited number of tests for each bolt size has, particularly in the larger diameter bolt thread, caused a large spread. Some of the average points were found on the basis of two tests. However, these limited tests indicate that flake laminates have the possibility of being used as a load-transferring material from a concentrated load into a fiberglass structure.

From these few tests it appears that the use of flake laminates as an insert or additional reinforcing material for filament reinforced plastic is feasible. The pullout strength of the laminate is not as good as that of an aluminum plate, however, the flake laminate has the definite advantage of having a modulus which is near that of a filament wound composite.

TABLE XX

THREAD STRENGTH IN GLASS FLAKE LAMINATE

70-30 Flake Laminate - .36" thick

Bolt Size	Load (lbs)	Load/Thread (lbs)
1/2 - 13		
1	3240	624
2	2525	540
10	2325	496
Average		554
3/9 - 16		
3	2555	444
4	3550	616
Average		530
1/4 - 20		
5	1815	252
	2050	285
Average		268
10 - 24		
7	1650	191
8	1780	204
		198

TABLE XXI

THREAD STRENGTH IN GLASS FLAKE LAMINATE

Laminate thickness = 0.68"

Bolt Size	Total Load (lbs)	Load/Thread (lbs)	Remarks
1/2 - 13	8700	1000	
5/16 - 18	6120	524	Hole parallel to flake
5/16 - 18	4500	410	Hole perpendicular to flake

TABLE XXII

THREAD STRENGTH IN ALUMINUM PLATE

Bolt Size	Load (lbs)	Plate Thickness	Total Thread	Load/Thread (lbs)
1/2 - 13	12100	.50	6.5	1870
3/8 - 16	8200	.25	4	2050
1/4 - 20	5060	.25	5	1010
10 - 24	4000*	.25	6	667+

* Bolt Failure

These tests indicate that there is possibly an optimum bolt diameter for a given laminate thickness. This assumes that the tapped thread used is the standard coarse series. The tests showed that in this case the thicker material developed a greater load per thread than the same bolt thread in a thinner material. Another factor which determines the thread strength is that of the number of threads per inch. The tests indicated that the decrease in strength was not as great for a flake laminate as it was for an aluminum plate, when the bolt diameter decreased and the number of threads per inch increased.

The wide variations in thread strength indicated that fabrication variations will have an effect upon the strength of the thread. The effect of stress concentration was not determined in this evaluation. The curves in Figure 22 were calculated on the basis of the tensile strength, although the threads in the laminate appeared to have a tensile-shear type of failure. This type of failure would be reasonable for a flake laminate since the tensile strength is the weakest strength.

The use of the tensile strength showed a conservatively calculated bolt strength, since most of the test points fall above the curve.

VIII. ROCKET NOZZLE EROSION RATE

Flake rocket nozzle specimens were tested to determine their erosion rate when exposed to the exhaust of Narmco's hydrogen-oxygen rocket motor. The erosion rate is measured by recording the instantaneous pressure within the motor's combustion chamber. Then, since the chamber pressure is inversely proportional to the throat or orifice area, the rate of change of orifice area can be found. As long as the throat remains circular as it erodes, the rate of change of the throat diameter can also be found.

The resin used in these tests was Narmco's Metlbond 2021 high temperature adhesive. One specimen was 95% flake, two were 85%, and two were 75% flake by weight. The data are summarized in Figures 23 and 24. Note in Figure 24 that there is a gap in which no measurements have been made. Unfortunately, it appears that the erosion rate approaches a minimum somewhere in this gap between zero flake content and 75% flake content. However, these measurements do not indicate any advantage to flake composites for this application.

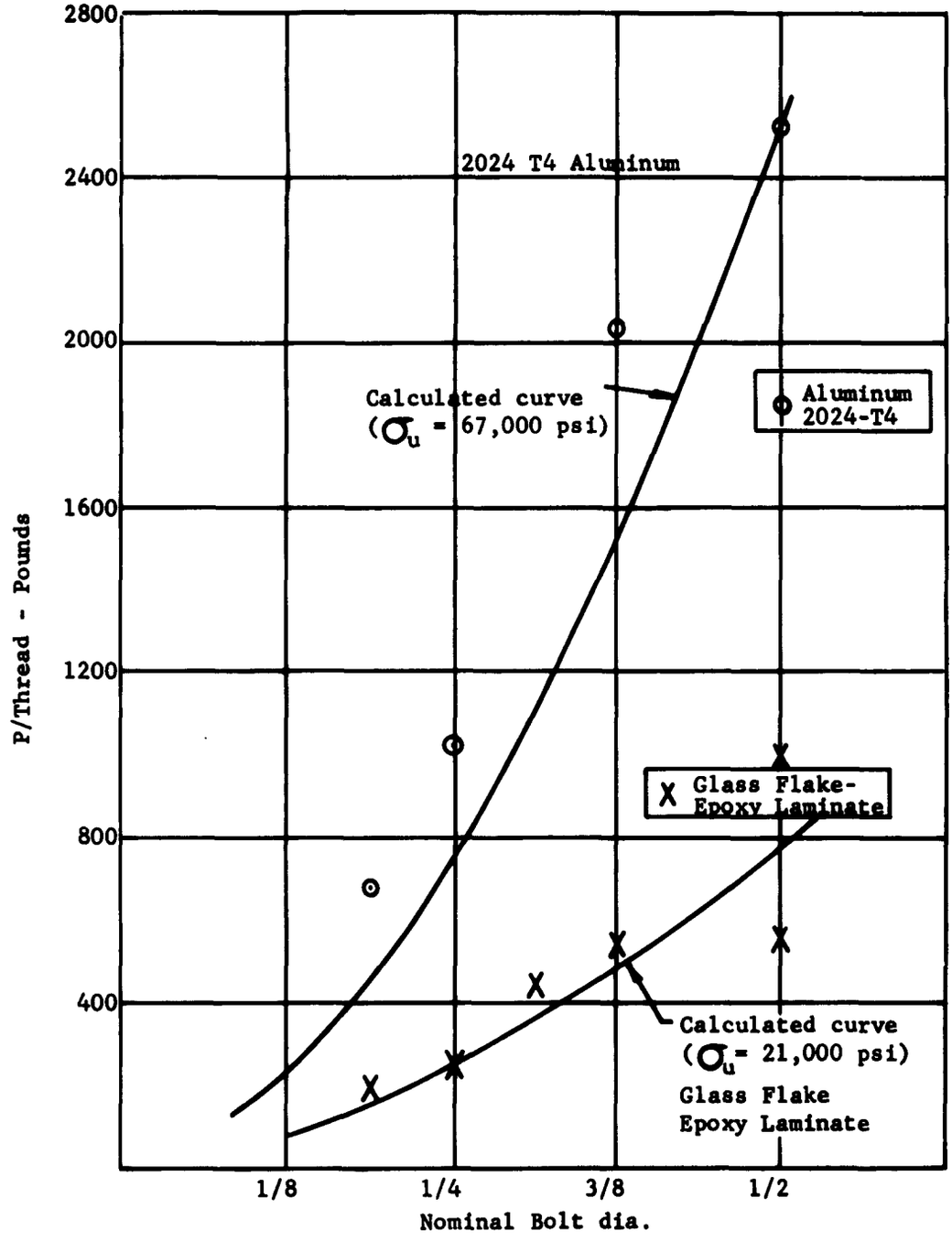

Figure 22. Load/Thread vs. Bolt Diameter

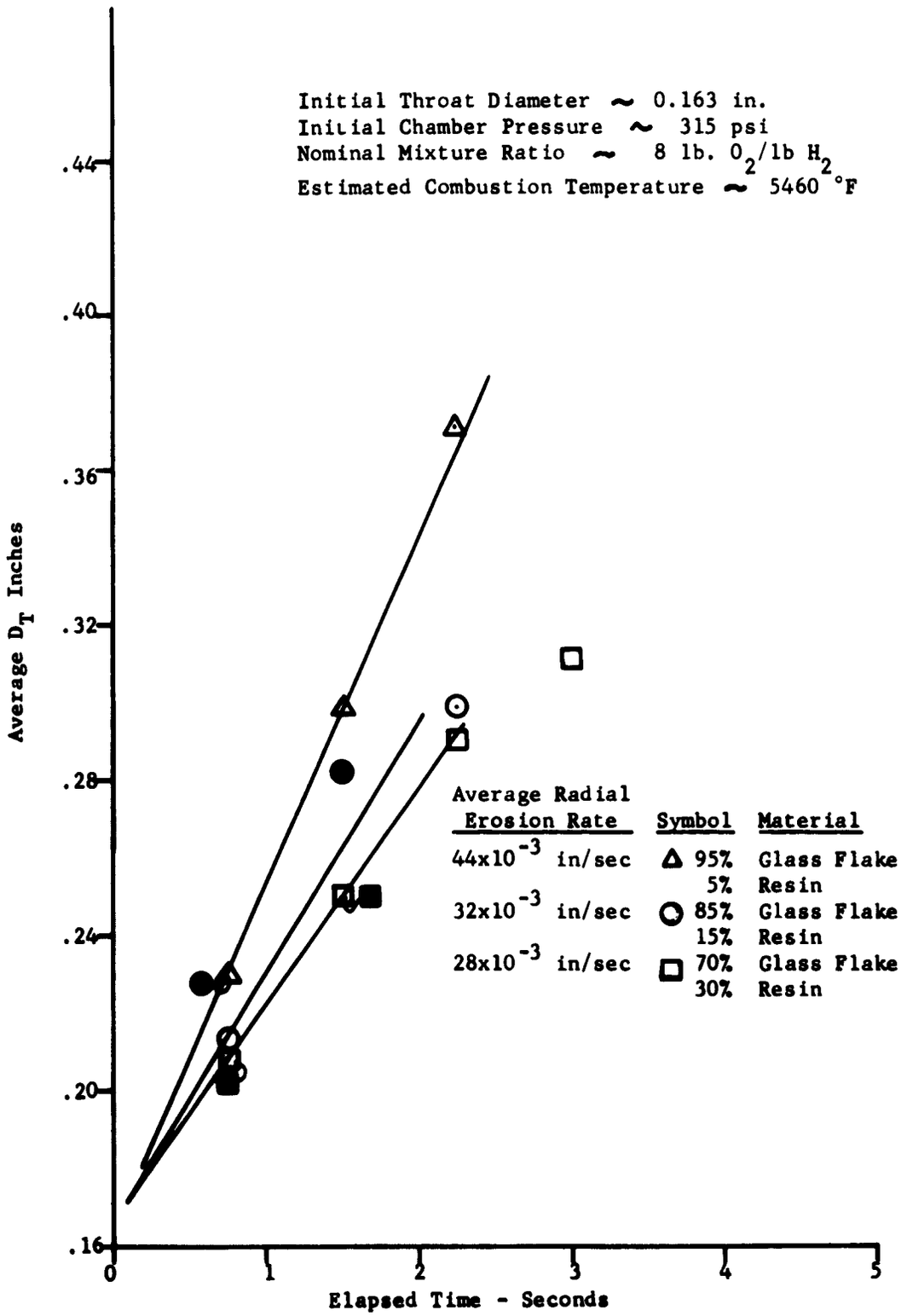

Figure 23. H_2 - O_2 **Rocket Nozzle Tests, Throat Diameter Erosion**

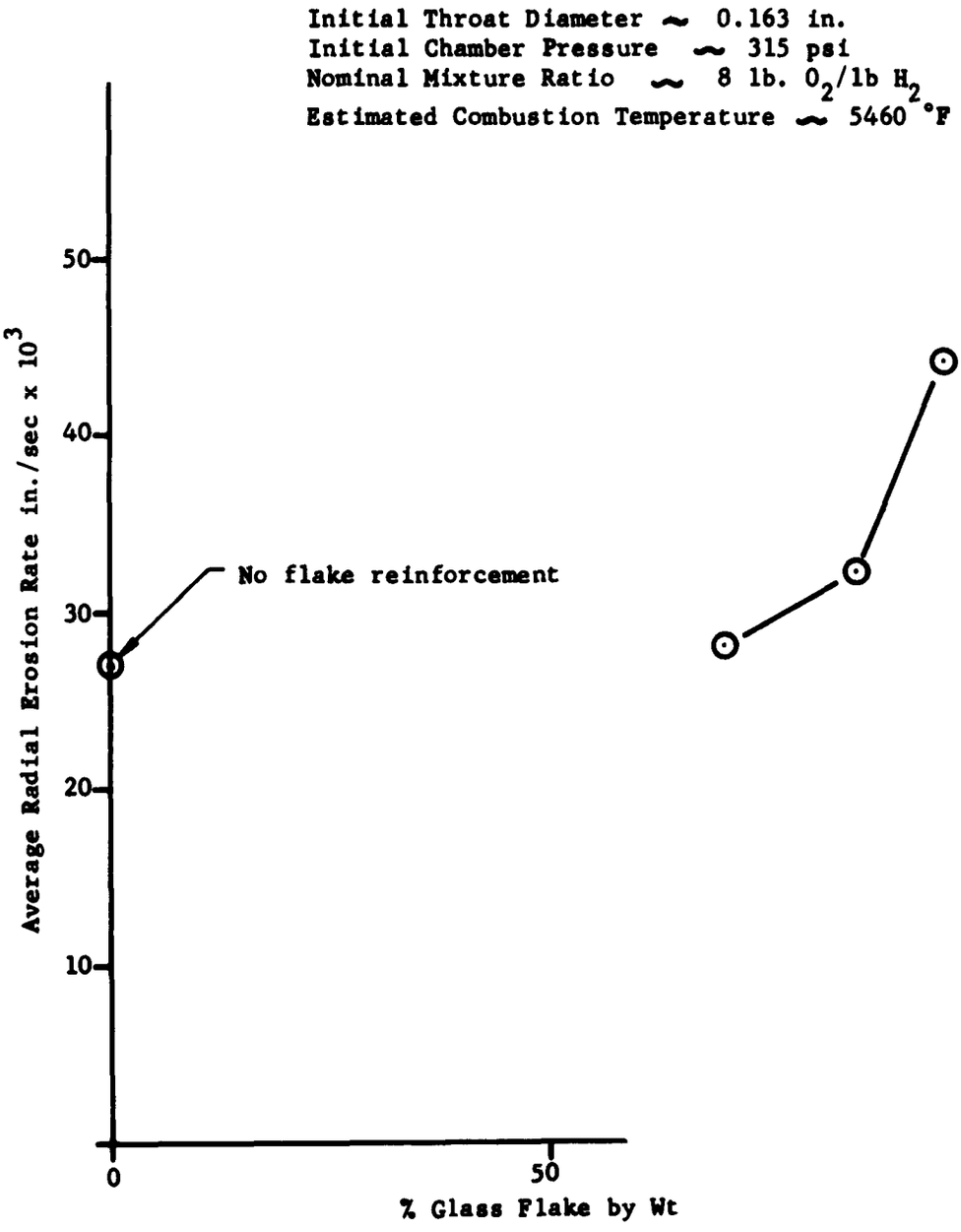

Figure 24. H_2 - O_2 Rocket Nozzle Tests, Thi

IX. SUMMARY OF THEORETICAL INVESTIGATIONS

A. The Determination of the Stresses in the Lap Joints of Circular Shaped Plates by the Method of Conformal Mapping

Although past examinations have reviewed and evaluated the methods of load transferal from flake to flake, the methods used were restricted to assumptions of uniform shear, no flake bending, and the absence of concentration effects. After comparing theory with experiment, it was determined that concentration effects in the lap joint must assert a large influence on the total load carrying capability of such a composite. This influence is particularly great when the composite undergoes tensile loads. Therefore, the problem of concentrated stresses in circular lap joints was evaluated. The method developed for evaluating these stress concentrations is presented in the Appendix of Quarterly Progress Report No. 2.

The theoretical results show that the concentrated stresses decrease with the increasing of the lap angle if the applied tensile forces and the flexural rigidity of plates hold constant. This agrees with the experimental data qualitatively, but varies in magnitude in the regions where the concentrated stresses occur. This quantitative disagreement is the result of experimental models, deviating of necessity, from the mathematical model.

A typical stress distribution is shown in Figure 25. For a corresponding overlap joint, the stress points are shown by letters on the flake diagram in Figure 26. As can be seen from Figure 25, the radial stress near the edge of the flake intersect reaches a factor of eight times the uniform stress in the flake. This indicates that when the failing stress of the flake material is reached at the edge and failure is initiated, the input stress in the flake is at least eight times less than the material strength. Therefore, if the glass flake has a strength capability of 160,000 psi, its maximum possible transferal stress would be only 20,000 psi in tension. When spacing and other factors are added to this figure, then the experimental results that have been obtained indicate that the tensile strength of the individual flakes must be in excess of 300,000 psi.

This concentration effect, of course, is not as dramatically apparent when the composite is in compression. Although the stress concentration effect is still in existence, the basic material strength is higher in compression and, even if material failure is achieved, the load can still be transferred through material bearing capabilities. However, it is felt that this concentration effect is indicated in the present experimental stress levels determined for compression and tension of glass flake composites.

Figure 27 shows these edge concentration effects on a small overlap angle, using photoelastic methods. Figure 28 demonstrates the failure pattern resulting from failure initiated by these stress concentrations. Figure 29 demonstrates the same concentration effects in a larger overlap angle; however, the magnitude of stress concentration is not as great. These flakes were actually 6" diameter, E glass plates, bonded and tested in

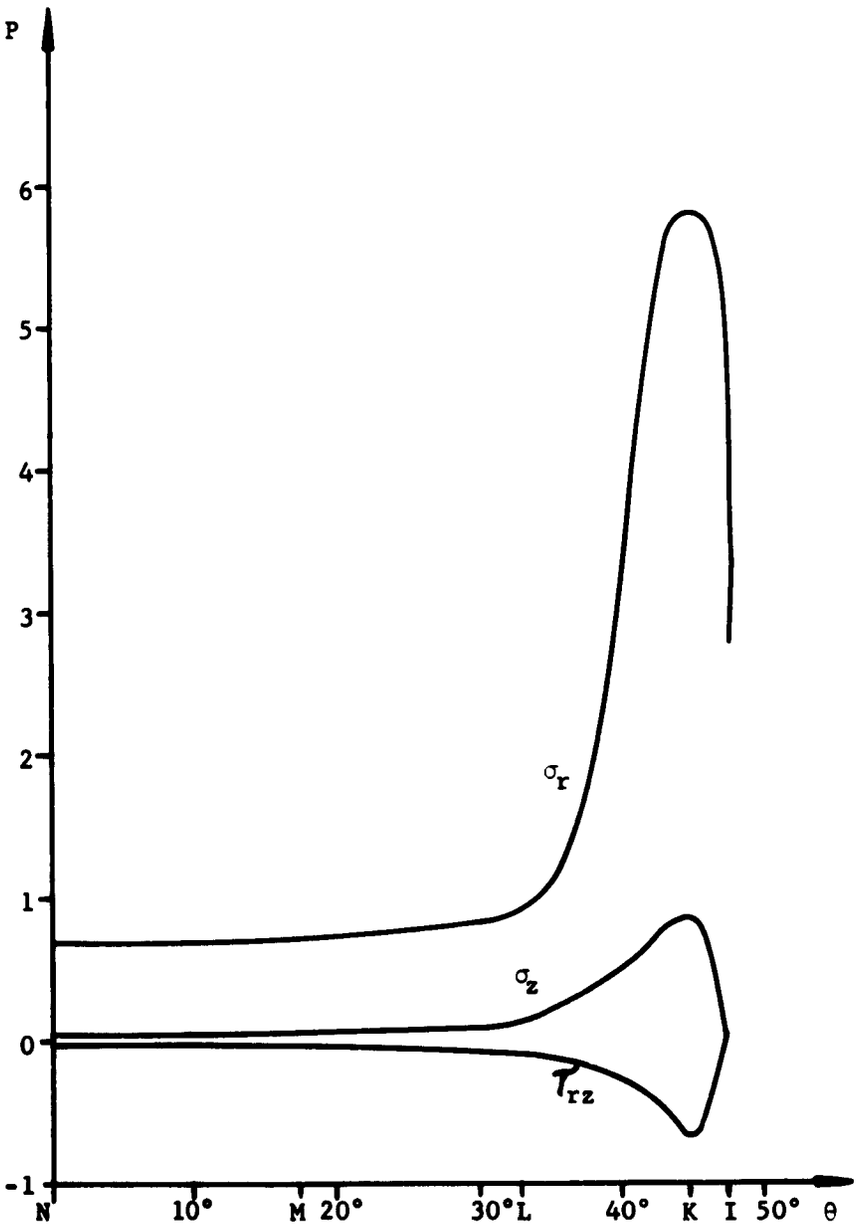

Figure 25. Stress Distribution Along the Circular Arc NMLKI

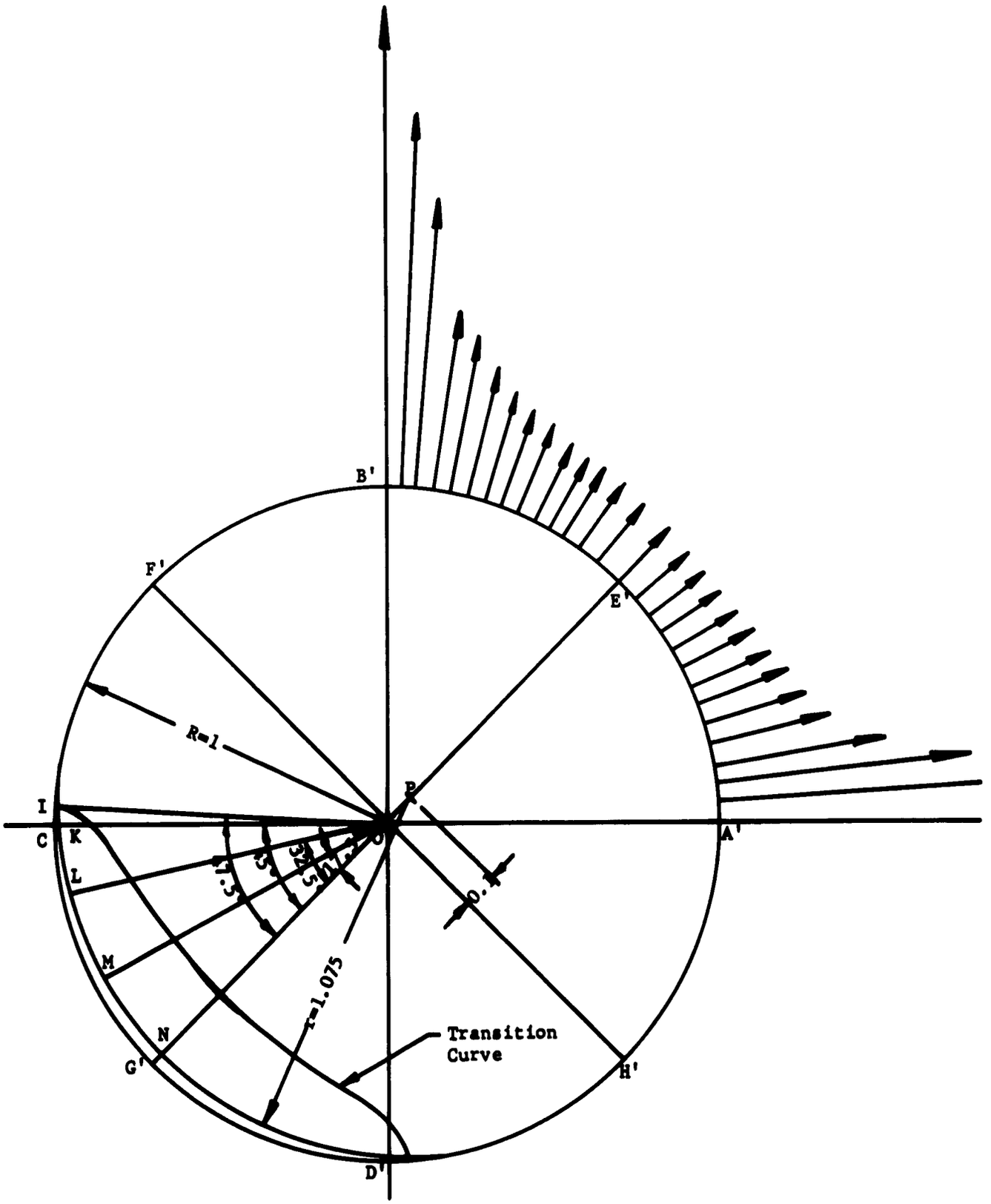

Figure26. Radial Forces Applied to Lap Joints of a Unit Circular Plate And The Plate With Transition Curve as a Part of its Edges

Figure 27. Stress Concentration in Small Overlap Angle

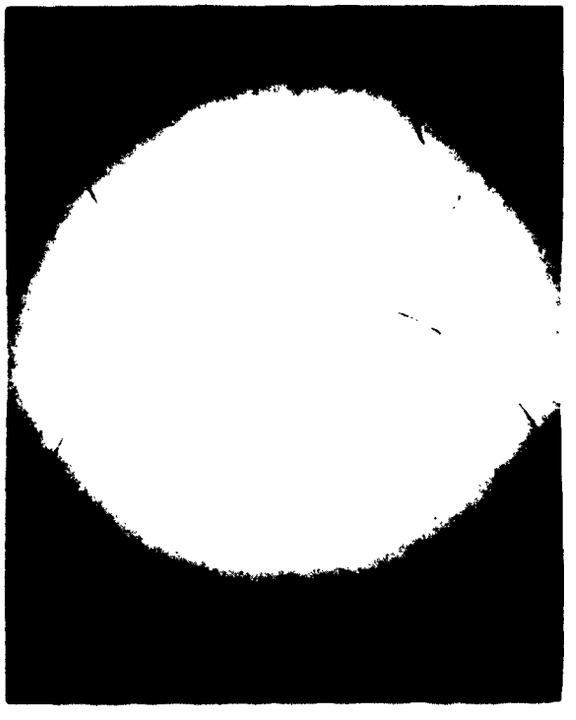

Figure 28. Failure Pattern of Small Overlap Angle

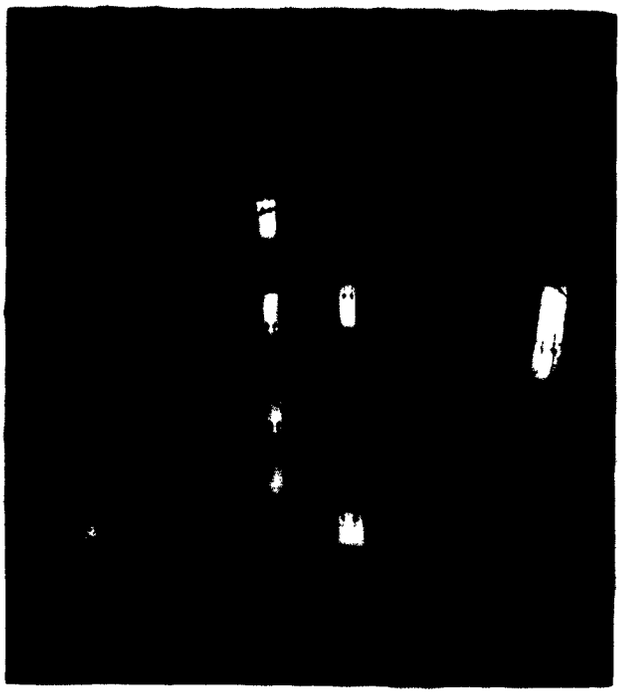

Figure 29. Stress Concentration in Large Overlap Angle

Narmco's Tinius-Olsen testing machine. It is believed that scale factor will have a limited effect on concentration factors.

B. A Review of Theories of Solid and Composite Beams*

Elementary theory of bending has been reviewed from the literature. It is shown that for span-to-depth ratios larger than 10, the error in deflection based on elementary theory will be negligible. Based on published data, it is recommended that the ratio of width-to-depth also be kept small, because for a ratio of one, the error in maximum stress is about 10% for a cantilever beam.

The elementary theory of bending for a homogeneous beam is modified for a composite beam. An expression for flexural rigidity has been derived for a composite beam. This value could be used in the expression of elementary theory of bending.

---

* See Appendix to Quarterly Progress Report No. 3 for this contract.

C. A Comparitive Study of Ultimate Strength of a Given Composite Reinforced Either by Flakes or Fibers or by Flake-Fiber Combinations Under Bending and Compressive Loads

This work was done in an effort to theoretically determine the advantages of flake-fiber composites. The complete study conducted in the two month extension period of the program is presented in the Appendix of this report. It was concluded that if glass flake is required to be used in structural components for reasons other than structural, (e.g., impermeability or as a notch arrester) the strength property can be improved by the addition of glass fibers to the composite.

X. SUMMARY AND CONCLUSIONS

In this program the fundamental work conducted during the first year was advanced in detail and advantageous applications of flake composites were investigated. Perhaps the most promising application of flake is in flake fiber combinations, since these composites are at least as strong as fiber glass composites and have a high modulus of elasticity, extremely low water and gas permeability, and good electrical properties.

The theoretical work conducted during the period covered by this report predicted inherent stress concentrations of up to eight times the nominal stress in circular flake composites. This is verified by the low hole and notch sensitivity of flake material and by the theoretical work conducted during the first year of the program.

From the investigation of techniques of fabricating flake cylinders it is indicated that the use of flake as a laminating material has potential. In an extensive Air Force program conducted at Narmco entitled, "Molded Flake Composites," (see Final Summary Report, Contract No. AF33(616)-7195) flake composites were compression molded with matched molds in a variety of simple configurations. The results indicated very little potential for this method of fabrication. However, it is believed that with the use of preformed or b-staged sheets of flake composite and fluid molding pressure, successful fabrication techniques can be developed.

APPENDIX

A COMPARATIVE STUDY OF ULTIMATE STRENGTH OF A GIVEN COMPOSITE REINFORCED EITHER BY FLAKES OR FIBERS OR BY FIBER-FLAKE COMBINATION UNDER BENDING AND COMPRESSIVE LOADS

APPENDIX

A COMPARATIVE STUDY OF ULTIMATE STRENGTH OF A GIVEN COMPOSITE REINFORCED EITHER BY FLAKES OR FIBERS OR BY FIBER-FLAKE COMBINATION UNDER BENDING AND COMPRESSIVE LOADS

The ultimate strength of a composite depends upon the mechanical properties of both the matrix and reinforcing materials. Reinforcing materials behave differently for various loading conditions. Hence, a comparative study will be made on the ultimate strength of a given cross section of composite reinforced either by flakes or fibers, or by fiber-flake combination, under bending and compressive loads.

The following assumptions will be made in the derivation of theoretical relations:

1. Glass flakes and resin are uniformly mixed and physical properties of a glass flake resin composite can be assumed to be constant.

2. Glass fibers are uniformly distributed in a matrix and oriented in the direction parallel to the longitudinal axis of the laminate.

3. Each of resin, glass fibers, and flake-resin composite obeys Hooke's law.

4. There is no sliding at the interface of two different materials.

5. The laminate is straight, prismatic, and unstrained before loading.

It is noted that the second assumption does not involve average physical properties of a fiber-reinforced lamination in calculation.

In the present analysis a flake resin composite and two composite laminates, as shown in Figure 25, will be considered. The number of fibers in any fiber-reinforced lamination is denoted by n.

I. COMPRESSION

If Young's moduli of resin, glass fibers, and flake-reinforced composite are denoted by E_r, E_F, and E_f, respectively, the stiffness of any cross section of the fiber-reinforced laminate (Figure 25b) is given by

$$(EA)_b = bhE_R + 3n\pi r^2 (E_F - E_R) \qquad (1)$$

where r is the radius of glass fibers.

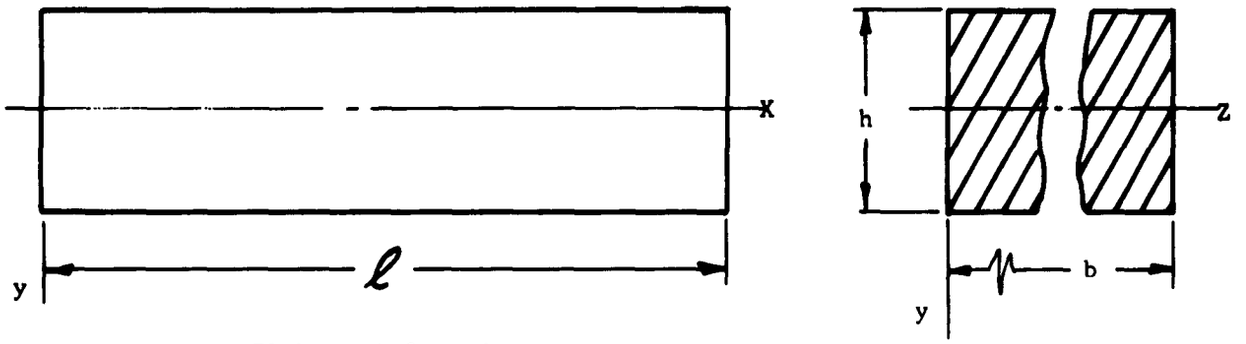

a. A Flake-Reinforced Composite

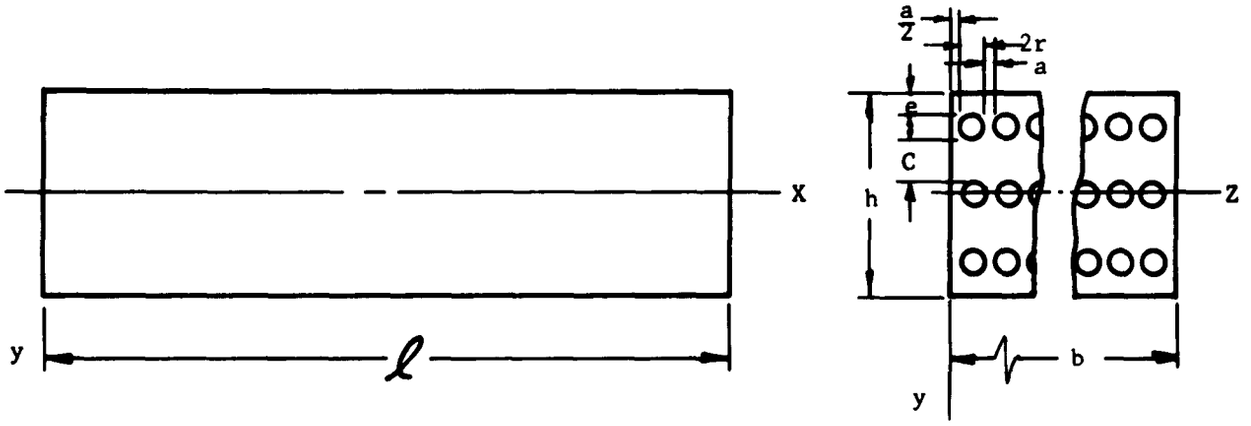

b. A Fiber-Reinforced Laminate

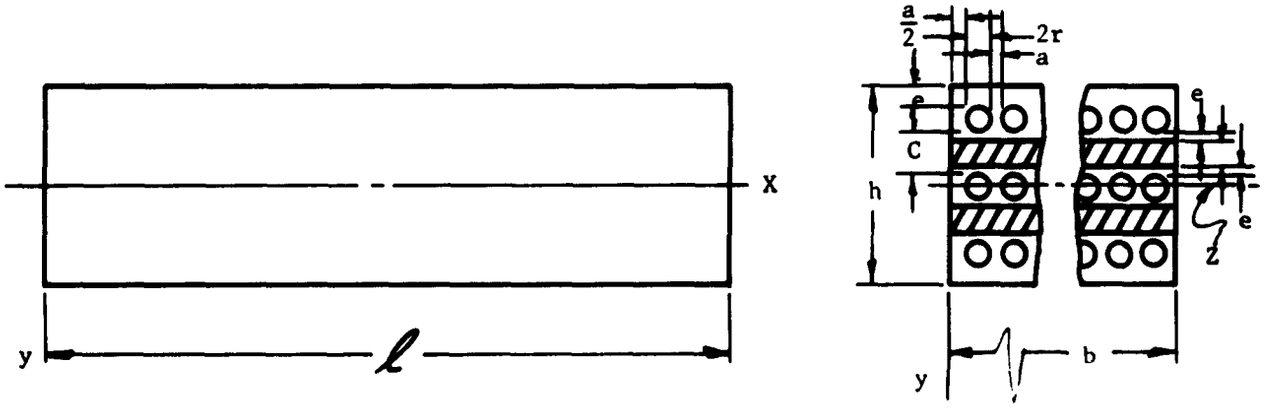

c. A Flake-and-Fiber-Reinforced Laminate

Figure 30. Three Types of Composites

The axial strain of the laminate is

$$\epsilon_b = - \frac{P_b}{(EA)_b} \tag{2}$$

where P_b is the axially applied compression uniformly distributed at the ends.

Then the stresses of fiber and resin are respectively given by

$$(\sigma_F)_b = E_F \epsilon_b \tag{3}$$

$$(\sigma_R)_b = E_R \epsilon_b \tag{4}$$

Similarly, the flake-and-fiber-reinforced laminate (Figure 25c) is subjected to a compressive force of P_c. The stiffness for this cross section is given as

$$(EA)_c = (EA)_b + 2b\,(c-2e)(E_f-E_r) \tag{5}$$

$$\epsilon_c = - \frac{P_c}{(EA)_c} \tag{6}$$

$$(\sigma f)_c = E_f \epsilon_c \tag{7}$$

$$(\sigma_F)_c = E_F \epsilon_c \tag{8}$$

$$(\sigma_R)_c = E_R \epsilon_c \tag{9}$$

where $(EA)_c$, ϵ_c, and $(\sigma_f)_c$ are stiffness and axial strain of the laminate and axial stress of the flake-reinforced lamination.

Since the flake-reinforced composite (Figure 1a) is assumed to be isotropic, the axial stress of this composite under compressive force P_a is

$$(\sigma_f)_a = - \frac{P_a}{ht} \tag{10}$$

Then compressive stresses or the maximum compressive loads for these three cases, as shown in Figure 25, can be calculated by using equations (3), (4), (7), (8), (9), and (10) for any given compressive force and set of dimensions. The values of E_r, E_F and E_f are different from one another. For given values of (r) radius of the fibers, and the cross-sectional dimensions (b and h) of the composite, the number of fibers (n) and the spacings of fibers (c and e) in equations 1 and 5 can be adjusted so that the stiffness of the laminate is as large as possible. With the increase of stiffness the ultimate load carried by a composite will be increased as seen from equations 2, 6, and 10.

For example, the following Young's moduli and ultimate compressive stresses are assumed

$$E_R = 0.45 \times 10^6 \text{ psi}, \quad (\sigma_u)_R = 10 \times 10^3 \text{ psi}$$

$E_F = 10.5 \times 10^6$ psi, $(\sigma_u)_F = 150 \times 10^3$ psi

$E_f = 5.92 \times 10^6$ psi, $(\sigma_u)_f = 53 \times 10^3$ psi

and the values of b, h, n and e are assumed as

$b = 25r$, $h = 18r$

$n = 10$, $e = 0$

where the radius of fibers r is in inches.

From Figure 25b or c we have

$c = 6r$

If the ultimate strain and the maximum load which can be applied to a single material in the composite are denoted by E_u and P_{max}, the numerical results obtained by using equations (1) thru (10) are shown in Table XXIII.

TABLE XXIII

COMPARISON OF MAXIMUM COMPRESSIVE LOADS IN DIFFERENT COMPOSITE

Structures and Materials	Flake-Reinforced Composite	Fiber-reinforced Laminate		Flake- and Fiber-Reinforced Laminate		
		Resin	Fiber	Resin	Flake Reinf Composite	Fiber
$\epsilon = \sigma_u/E$	-.00895	-.02222	-.01429	-.02222	-.00895	-.01429
(EA)	$26.6 \times 10^8 r^2$	$11.5 \times 10^8 r^2$		$27.9 \times 10^8 r^2$		
$P_{max} = -\epsilon_u (EA)$	$.238 \times 10^8 r^2$	$.255 \times 10^8 r^2$	$.164.10^8 r^2$	$.620 \times 10^8 r^2$	$.250 \times 10^8 r^2$	$.399 \times 10^8 r^2$

The values of P_{max} show that the maximum applied load of the flake-and-fiber-reinforced laminate is at least 0.05 times larger than that of the flake-reinforced beam and 0.52 times larger than that of the fiber-reinforced laminate.

II. BENDING

The flexural rigidity of a laminate as shown in Figure 25b or c has to be determined before calculating bending stresses produced by applied bending moment or lateral forces. By using geometrical relation with the assumption that any plane section of a laminate remains plane after bending the strain ϵ, at a distance y from the neutral axis could be written as

$$\epsilon = \frac{y}{R} \qquad (11)$$

where R is the radius of curvature of the laminate after bending.

If each of materials of the laminate obeys Hooke's law, the bending stresses are, for small deflections, given by

$$\sigma_R = E_R \varepsilon = - E_R y \frac{d^2y}{dx^2} \tag{12}$$

$$\sigma_F = E_F \varepsilon = - E_F y \frac{d^2y}{dx^2} \tag{13}$$

$$\sigma_f = E_f \varepsilon = - E_f y \frac{d^2y}{dx^2} \tag{14}$$

where σ_R, σ_F, and σ_f are bending stresses in resin, fibers, and flake-resin composite at a distance y from the neutral axis of the laminate respectively.

The internal moment, M_b, produced by bending stresses over a cross section of the fiber-reinforced laminate (Figure 30b) is

$$M_b = 2\int_0^{\frac{h}{2}} y \sigma_R b dy + 4n\left[\int_0^r y(\sigma_F-\sigma_R)\sqrt{r^2- y^2}\ dy + \int_{r+c}^{3r+c} y(\sigma_F-\sigma_R)\sqrt{r^2-(y-2r-c)^2}\ dy\right] \tag{15}$$

It can be seen that the first integral on the right-hand side of equation (15) represents the moment due to the whole beam made up of resin only, and the other two integrals represent the effect of replacing the resin by fibers on the moment. Substituting equations (21 and (13) in (15) and performing the integrations yield

$$M_b = - (EI)_b \frac{d^2y}{dx^2} \tag{16}$$

where $(EI)_b$ is the flexural rigidity of the laminate given by

$$(EI)_b = E_R I_Z + 2n\pi r^2 (E_F-E_R)\left[\frac{35}{3} r^2 + 4rc + c^2\right] \tag{17}$$

with I_Z being the moment of inertia of the whole cross section with respect to its neutral axis.

Similarly, the internal moment, M_c for the flake- and fiber-reinforced laminate (Figure 30c) is

$$M_c = M_b + 2\int_{r+e}^{r+c-e} y(\sigma_f-\sigma_R)b\ dy \tag{18}$$

By following a similar calculation equation (18) becomes

$$M_c = -(EI)_c \frac{d^2y}{dx^2} \tag{19}$$

where $(EI)_c = (EI)_b + \frac{2}{3} b (E_f - E_R) \left[(r+c-e)^3 - (r+e)^3\right]$ (20)

It is understood that the following assumptions have been also made in deriving equations (17) and (20).

(a) The effect of shearing forces on the curvature of the deflection curve can be neglected.

(b) The materials in the neutral plane do not undergo strains during bending.

The bending strain ε_x at a distance y from the neutral axis of a cross section (Figure 30 b or c) is

$$\varepsilon_x = \frac{M y}{(EI)} \tag{21}$$

where M and (EI) are applied bending moment and flexural rigidity of the laminate.

Then the bending stress of any material at a distance y from the neutral axis can be determined by using equation (21) with Hooke's law.

Since the flake-reinforced beam (Figure 30a) has been assumed to be isotropic the stresses of the beam due to bending moment M are

$$(\sigma_x)_f = \frac{M y}{I_Z} \tag{22}$$

Thus bending stresses for the cases as shown in Figure 30 can be calculated by using Hooke's law and equations (21) and (22) for any given set of dimensions of beam and applied bending moment. Reversely the maximum bending moment which can be applied to the beam can be determined by using these equations.

For numerical example we assume that the values of b, h, n, e, and c Young's moduli, and ultimate tensile stress of resin, glass fibers, and flake-reinforced composite are the same as those given in the previous example except the ultimate tensile stress of the flake-reinforced composite is assumed to be

$$(\sigma_u)_f = 21 \times 10^3 \text{ psi}$$

If the maximum bending moment which can be applied to a single material at the most center surface of the beam (Figure 30) is denoted by M_{max}, the numerical results obtained by using equations (17), (20), (21) and (22) are shown in Table XXIV.

TABLE XXIV

COMPARISON OF MAXIMUM BENDING MOMENTS IN DIFFERENT COMPOSITES

Structures and Materials	Flake-Reinforced Beam		Fiber-Reinforced Laminate		Flake- and Fiber-Reinforced Laminate	
	Tens.	Comp.	Resin	Fiber	Resin	Fiber
$\epsilon_u = \sigma_u / E$			.02222	.01429	.02222	.01429
I_Z	$12.15 \times 10^3 r^4$		$12.15 \times 10^3 r^4$		$12.15 \times 10^3 r^4$	
(EI)			$5.08 \times 10^{10} r^4$		$8.20 \times 10^{10} r^4$	
M_{max}	$.28 \times 10^8 r^3$	$.72 \times 10^8 r^3$	$1.25 \times 10^8 r^3$	$.81 \times 10^8 r^3$	$2.02 \times 10^8 r^3$	$1.30 \times 10^8 r^3$

The values of M_{max} show that the maximum applied bending moment of the flake- and fiber-reinforced laminate is 3.64 times larger that of the flake-reinforced beam and 0.6 times larger than that of the fiber-reinforced laminate.

In conclusion it can be said that if glass flake is required to be used in structural components for reasons other than strength requirements, for example impervious or as a notch arrester, the strength property can be improved by the addition of glass fibers in this composite.

Prepared by: _____
D. Stevens

Approved by: _____
Dr. F. Riel

_____
Dr. S. Yurenka

DISTRIBUTION LIST - Contract NOw 61-0305-c

Picatinny Arsenal
Dover, N. J.
Attn: Mr. J. Matlack, Chief Plastics

NA&SA
Langley Research Center
Langley, Virginia
Attn: Mr. Ross Levine, Structures Group

Ordnance Materials Research Office
Watertown Arsenal
Watertown 72, Mass.
Attn: Mr. Irving Kahn

Office of Naval Research
T-3 Bldg. 17th & Constitution Ave. N.W.
Washington 25, D. C.
Attn: Dr Harold Liebowitz

Boeing Aircraft Company
Box 2976
Seattle, Washington
Attn: Mr. L. J. Workman

Office, Chief of Ordnance
Department of the Army, Washington 25, D. C.
Attn: ORDTB Mtls.

Chief, Bureau of Ships
Washington 25, D. C.
Attn: Code 342 (John Alfers)

Material Laboratory
N. Y. Naval Shipyard
Brooklyn 1, N. Y.
Attn: Code 948

Engr. R. & D Laboratories
Corps of Engineers
U. S. Army
Ft. Belvoir, Virginia

U. S. Naval Ordnance Laboratory
White Oak, Silver Spring, Md.
Attn: Dr. A. Lightbody

Owens-Corning Fiberglas Corp.
806 Connecticut Avenue, N. W.
Washington, D. C.
Attn: Mr. R. J. Weaver

U. S. Naval Research Laboratory
Washington 25, D. C.
Attn: Code 6210 (Mr. Joe Kies)

Chief, Bureau of Naval Weapons (11 cys)
Washington 25, D. C. (1 reproducible)
Attn: Code RRMA-31 (P. R. Stone)
Via: Inspector of Naval Material
Los Angeles, California

Aeronautical Systems Division
Wright-Patterson AFB, Ohio
Attn: WCLTEM

Aeronautical Systems Division
Wright-Patterson AFB, Ohio
Attn: WWRCWC-1

Aeronautical Systems Division
Wright-Patterson AFB, Ohio
Attn: WCLTEC

Chief, Bureau of Naval Weapons (12 Cys)
Washington 25, D. C.
Attn: DLI-311 (for file & release to ASTIA)

Commander
Aeronautical Systems Division
Wright-Patterson AFB, Ohio
Attn: LMEMC, Lt. W. Messenger

Office of Director of Defense (2 cys)
Research & Engineering
PLASTEC
Picatinny Arsenal
Dover, N. J.
Attn: Mr. Harry E. Plbly, Jr.

Forest Products Laboratory
Madison 5, Wisconsin
Attn: Dr. Don Brouse

NORAIR, A. Div. of Northrop Corp.
1001 E. Broadway
Hawthorne, California
Attn: Mr. A. P. Binsacca, Supvr.,
Matls & Process Engineering

DISTRIBUTION LIST (cont'd) - Contract NOw 61-0302-c

U. S. Rubber Company
1700 E. Street, N. W.
Washington 6, D. C.
Attn: Mr. J. W. DeVorss

NA&SA
Lewis Research Center
21000 Brookpark Rd.
Cleveland 35, Ohio
Attn: Library

Lockheed Aircraft Corp.
California Division
Burbank, California
Attn: E. A. Green,
Production Engr. Dept.

Commander
U. S. Naval Ordnance Test Station
China Lake, California
Attn: Mr. S. H. Herzog

Hdqs., A. F. Systems Command
Aeronautical Systems Division
Wright-Patterson AFB, Ohio
Attn: ASRCEM-2 (T. J. Reinhart)

Electric Boat Division
General Dynamics Corp.
Groton, Conn.
Attn: Robinson Research Library

Pittsburgh Plate Glass Co.
Glass Research Center, Box 11472
Pittsburgh, 38, Pa.
Attn: R. M. Watterson, Librarian

Houze Glass Corp.
Point Marion, Pa.
Attn: R. M. Pattison

Bureau of Naval Weapons
Special Projects Division
Attn: Mr. Harold Bernstein

Aerospace Industries Assn. (2 cys)
Shoreham Bldg.
Washington, D. C.
Attn: Mr. J. P. Reese

U. S. Navy (12 cys)
Tech. Data Division
(TD-4106)
Washington 25, D. C.